47. CRETACEOUS FORMATIONS FROM THE LOWER CONTINENTAL RISE OFF CAPE HATTERAS: ORGANIC GEOCHEMISTRY, DINOFLAGELLATE CYSTS, AND THE CENOMANIAN/TURONIAN BOUNDARY EVENT AT SITES 603 (LEG 93) AND 105 (LEG 11)[1]

J. P. Herbin, Institut Français du Pétrole
E. Masure, Département de Géologie Sédimentaire, Université Pierre et Marie Curie
and
J. Roucaché, Institut Français du Pétrole[2]

ABSTRACT

Geochemical characterizations of the Cretaceous formations at Site 603 are quite comparable with those at Site 105. In the Blake-Bahama and the Hatteras formations, the petroleum potential is medium (<5 kg HC/t of rock) to very low (<0.5 kg HC/t of rock), and the organic matter is mainly of type III origin, that is, terrestrial. At the top of the Hatteras Formation, there is a condensed series, which chiefly contains organic matter of type II origin, with up to 20 wt.% total organic carbon content in Core 603B-34 and 25 wt.% in Core 105-9. This accumulation corresponds to the Cenomanian/Turonian boundary event. An examination of dinoflagellates in the kerogen concentration assigns dates to the samples studied by organic geochemistry. The Cenomanian and Turonian age of the organic-matter-rich black claystones indicates a low rate of sedimentation, about 1 m/Ma. Furthermore, the occurrence of type II organic matter indicates an anoxic environment with insufficient oxygen renewal to oxidize the sinking hemipelagic organic matter. This organic enrichment is not related to local phenomena but to sedimentation over an extended area, because deposits are well known in various areas with different paleodepths in the North Atlantic.

INTRODUCTION

Hole 603B was drilled in 4642 m of water on the lower continental rise, 270 n. mi. east of Cape Hatteras (Fig. 1). The depositional history of Hole 603B was influenced by coastal oceanic events, whereas Site 105, only 68 n. mi. to the southeast (5251 m water depth), showed mainly pelagic influences.

At Site 105, three formations were found in the Cretaceous deposits:

1. The Blake-Bahama Formation (Hauterivian–Barremian), consisting of alternating dark marlstones and limestones.

2. The Hatteras Formation (Aptian–Albian–lower Cenomanian), consisting of alternating green and black shales.

3. The Plantagenet Formation (Senonian), composed of multicolored claystones.

In Hole 603B these formations occur in lithologic Units III, IV, and V. In addition, however, Hole 603B intersects a deep-sea fan which perhaps forms part of an apron of clastic-rich sediments of late Hauterivian–Barremian age along the lower continental margin of eastern North America.

Previous studies of Cretaceous deposits from DSDP sites in the North Atlantic (Graciansky et al., 1982; Herbin and Deroo, 1982; Müller et al., 1983) showed that an event corresponding to the upper Cenomanian/Turonian boundary existed between the Hatteras Formation and the Plantagenet Formation. This event, named variously the E2 Event, Cenomanian/Turonian Black Shales Horizon, or Cenomanian/Turonian Boundary Event (CTBE), is characterized by a level of laminated black claystones very rich in type II organic matter (15 to 40 wt.% of total organic carbon). The CTBE occurs along the different continental margins of the North Atlantic. Off the African continental margin it has been recognized at DSDP Sites 135, 137, 138, 367, and 368 as well as on the shelf in Senegal (Casamance area) or Morocco (Agadir–Tarfaya basins and Rif Mountains) (Herbin, Montadert, et al., in press; Thurow and Kuhnt, in press). Sites 398 and 551 off the European margin also give good opportunities to study the CTBE. However, off the American continental margin, only Site 105 up to now has revealed the presence of the CTBE in the western North Atlantic. Condensed deposits with a high total organic carbon content in Sections 105-9-3 and 105-9-4 mark the break between the Hatteras and the Plantagenet formations. The same phenomenon occurs over a longer interval in Sections 603B-34-1 to 603B-34-6.

This chapter has two sections. In the first, the results of detailed analyses of all of the Cretaceous formations in Hole 603B (lithologic Units III, IV, and V) will be discussed. In the second, the CTBE will be studied, first at Site 105 and then at Site 603.

METHODOLOGY

The amount of total organic carbon (TOC) was determined by a new methodology adapted to the Rock-Eval apparatus (Espitalié et al., 1984). After pyrolysis in an inert atmosphere, where the petroleum potential of the rock was determined (peaks S_1 and S_2), the rock was burned at about 600°C for 5 min. to determine the residual organic carbon content by detecting the CO_2 resulting from this combustion.

[1] van Hinte, J. E., Wise, S. W., Jr., et al., *Init. Repts. DSDP*, 93: Washington (U.S. Govt. Printing Office).

[2] Addresses: (Herbin, Roucaché) Institut Français du Pétrole, Direction de Recherche Géologie-Géochimie, B.P. 311, 92506 Rueil Malmaison Cedex, France; (Masure) Département de Géologie Sédimentaire Laboratoire de Micropaléontologie, UA 319, Université P. et M. Curie, 4, place Jussieu, 75230 Paris Cedex 05, France.

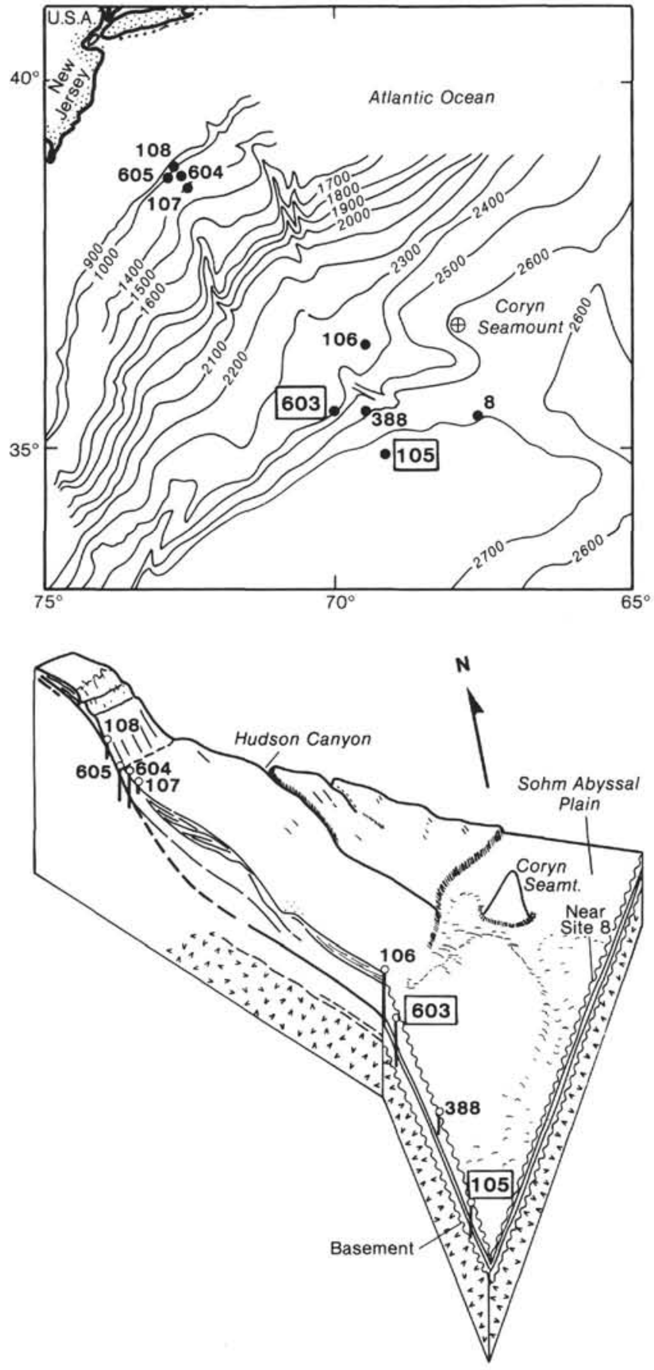

Figure 1. Section along the continental margin off New Jersey and location of Sites 105, 603, and other DSDP sites.

The total organic carbon content of the sample is the sum of the residual organic carbon and the pyrolyzed organic carbon. Under these conditions, the carbonates that are decomposed by a temperature below 600°C (siderite, nahcolite, dawsonite, etc.) are destroyed during the preceding pyrolysis and cannot interfere with the combustion of the residue, whereas decomposition of other carbonates (calcite, dolomite) is very low at 600°C during such a short (5 min.) combustion time.

Total organic carbon and Rock-Eval pyrolysis assays were performed on 436 samples. Among the 21 samples issued by the Organic Geochemistry Panel (Table 1), 13 with TOC of 0.5 wt.% were selected to be chloroform-extracted and analyzed by gas chromatography for their saturated hydrocarbons. Elemental analysis of the kerogen was performed on 11 samples. Since the preparation of the kerogen concentrates (Huc et al., 1978) was the same for the geochemical study and for the palynological study, both were performed in the interval containing the CTBE (Core 34) to characterize the type of organic matter and the age for the same rock.

RESULTS

Character of the Cretaceous Formations

Mineral Carbon and Carbonates (Table 1)

In the Blake-Bahama Formation, lithologic Subunit VB (Core 603B-82 to Section 603B-76-1, late Berriasian–Valanginian in age) is very rich in carbonates (8.5 wt.% of mineral carbon, i.e., 70 wt.% of $CaCO_3$), whereas in lithologic Subunit VA Section 603B-76-1 to Core 603B-44, Valanginian, Hauterivian, Barremian), the carbonate content is lower because of detrital input from the deep-sea fan (mineral carbon = 1.9 to 3.3, $CaCO_3$ = 15.8 to 27.5), except in Sample 603B-66-2, 135–137 cm (mineral carbon = 8.28, $CaCO_3$ = 68.9). Turbiditic siltstones are very poor in mineral carbon (0.63; $CaCO_3$ = 5.2).

Above the Blake-Bahama Formation, in the Hatteras Formation (Cores 603B-44 to -33, Aptian to Cenomanian–Turonian), the Plantagenet Formation (Cores 603B-33 to -22, Senonian), and even in the Bermuda Rise Formation (Cores 603B-22 to -15, Eocene), the mineral carbon is poor: 0.36 to 1.03 wt.%; 3–8.6 wt.% of equivalent $CaCO_3$.

The change from carbonate deposits in the Blake-Bahama Formation to the noncarbonate deposits of the overlying formations is a general feature of Cretaceous sedimentation in the North Atlantic realm, and corresponds to the E1 Event of Müller et al., 1983. This is interpreted as a rise in the carbonate compensation depth.

Organic Carbon (Table 1)

In the Blake-Bahama Formation the dark marlstones contain 0.6 to 2.9 wt.% TOC except in the more silty portions, where the TOC is very poor: 0.04 in Sample 603B-59-4, 127–127 cm. The green and reddish claystones of the Hatteras Formation (Samples 603B-38-3, 143–148 cm and 603B-43-4, 10–15 cm) are low in TOC content (0.04 and 0.03) whereas the dark claystones contain 2.7 to 3.4. A higher wt.% TOC is reached at the top of the Hatteras Formation (Cores 603B-34 and -33) with 4.6 to 20.4. This high enrichment is typical of the CTBE. Higher up in the reddish brown and green claystones of the Plantagenet Formation, the TOC content is very low (0.07 to 0.14). One sample of greyish claystone of Santonian age reaches 1.78 TOC.

The same pattern holds true for the Cretaceous formations at Site 105. In the Blake-Bahama Formation the average TOC is 1.5 wt.% (26 samples), in the Hatteras Formation it is about 2 (43 samples), and in the Plantagenet Formation it does not exceed 0.2. On the other hand, at the top of the Hatteras Formation, as in Hole 603B, the CTBE is recognizable from an enrichment in organic matter, with TOC up to 24.

Table 1. Geochemical data for the samples issued from the Organic Geochemistry Panel.

Core-Section (interval in cm)	Sub-bottom depth (m)	Formation	Age	Mineral carbon (%)	$CaCO_3$ (%)	TOC (%)	$S_1 + S_2$ (kg HC/t rock)	T_{max} (°C)	HI	OI	H/C	O/C	Pyrite (%)	Ash-free of pyrite (wt.%)	Extract/ rock (%)	Extract/ TOC (%)	Hydroatomic compounds (%)	Hydrocarbon fraction: Aromatic (%)	Hydrocarbon fraction: Saturated (%)	Pristane/Phytane
16-2, 140–143	968.30	Bermuda Rise	Eocene	0.70	5.8	0.10	0.70													
29-1, 57–62	1081.37		Santonian	0.36	3.0	1.78	0.64	440	34	40	0.67	0.27	25	2.8	0.022	1.2	67.8	5.2	27	1.41
29-3, 127–131	1085.07	Plantagenet		0.72	6.0	0.14	1.11													
33-2, 127–133	1121.27	(Unit III)	Turonian	0.75	6.2	0.07	0.37													
33-CC, 1–8	1127.49		Turonian	0.66	5.5	4.58	15.27	420	324	31	1.11	0.19	12	1.9	0.079	1.7	90.9	5.6	3.5	1.13
34-1, 82–83	1128.32	Cenomanian/Turonian	Turonian	1.02	8.5	20.40	104.30	412	485	26	1.23	0.18	28	2.5	0.387	1.9	94.3	4.2	1.5	0.78
34-3, 70–73	1131.20	Boundary Event	Cenomanian	0.84	7.0	10.71	43.34	415	396	40	1.19	0.17	42	2.0	0.207	1.9	94.	2.4	3.6	1.09
34-5, 23–25	1133.73		Cenomanian	0.90	7.5	7.79	28.86	416	355	30	1.15	0.15	32	1.9	0.125	1.6	94.1	3.3	2.6	0.84
35-3, 74–76	1140.24		Cenomanian	0.69	5.7	2.74	5.01	430	177	91	0.84	0.20	29	2.1	0.030	1.1	89.2	7.1	3.7	1.11
38-3, 143–148	1167.93	Hatteras	Albian	0.90	7.5	0.04	0.06													
43-4, 10–15	1209.40	(Unit IV)	Aptian	0.78	6.5	0.03	0.25													
44-1, 23–24	1214.63		Aptian	1.03	8.6	3.43	3.99	433	114	57	0.79	0.20	14	3.6	0.038	1.1	84.7	6.1	92	1.39
53-4, 135–139	1306.65		Barremian	3.30	27.5	2.27	0.95	423	39	81					0.032	1.4				1.39
59-4, 125–130	1364.15		Barremian	0.63	5.2	0.04	0.13													
66-2, 135–138	1426.55		Hauterivian	8.28	68.9	0.93	0.22	418	21	140	0.77	0.22	21	3.8	0.018	1.9				1.43
71-5, 125–130	1475.95	Deep-sea fan in	Hauterivian	2.88	24.0	1.46	0.31	424	13	90	0.66	0.24	22	2.9	0.016	1.1				1.68
{75-5, 17–19	1508.07	Blake-Bahama (Unit VA)	Valanginian	1.90	15.8	1.90	1.44	435	74	92	0.92	0.19	37	2.7	0.026	1.4	84.7	6.4	8.9	1.90
{75-5, 32–34	1508.22	Formation	Valanginian	2.51	20.9	2.51	1.56	436	61	57										
{75-5, 47–49	1508.37		Valanginian	2.63	21.9	2.63	2.99	433	111	64										
76-3, 125–130	1515.75	(Unit VB)	Valanginian	8.49	70.7	2.91	4.35	425	146	59					0.051	1.7				2.08
81-3, 124–129	1562.44		Valanginian	8.40	69.9	0.57	0.10	415	15	164	0.79	0.20	32	8.0	0.018	3.1				1.17

Note: TOC = total organic column; $S_1 + S_2$ = petroleum potential; HC = hydrocarbons; HI = hydrogen index (mg hydrocarbon compounds/g TOC); OI = oxygen index (mg oxygen compounds/g TOC); T_{max} = maximum temperature.

Pyrolysis Data (Table 1, Fig. 2)

Petroleum Potential (Table 1)

The petroleum potential is defined as the sum of Rock-Eval peak S_1 (corresponding to the free hydrocarbons in the rock) and peak S_2 (related to the hydrocarbons expelled during kerogen pyrolysis) (Espitalié et al., 1977). It is expressed in kilograms of hydrocarbons per metric ton of rock (kg HC/t). Five classes were considered: very good, more than 20 kg HC/t; good, 5.01 to 20.00; medium, 2.01 to 5.00; low, 0.51 to 2.00; and very low, 0.50 and less.

In the deep-sea fan of the Blake-Bahama Formation, the petroleum potential is very low to low except at the bottom. There, in samples of Valanginian age (Samples 603B-75-5, 47–49 cm and 603B-76-3, 125–130 cm), it reaches 3 to 4.3 kg HC/t. In the greyish claystones of the Hatteras Formation the petroleum potential is medium, 4 to 5. However, it is very low in the green and reddish claystones (0.06 to 0.25. At the top of the Hatteras Formation (Core 603B-34 and -33) the petroleum potential is good and even very good, with 4.6 to 104.3. This richness reflects the CTBE. This high content disappears in the multicolored claystones of the Plantagenet Formation (0.37 to 1.11) and in the overlying Bermuda Rise Formation (0.70)

Maturation (Table 1)

During pyrolysis of organic matter by Rock-Eval, the temperatures reached at maximum hydrocarbon production (T_{max}) for peak S_2 depend on both the stage of maturation and the nature of the organic matter (Espitalié et al., 1985). Vitrinite reflectance can be compared with the maturation scale derived from the Rock-Eval. A reflectance of 0.5%, which defines the boundary between immature and mature organic matter, roughly corresponds to T_{max} of 435°C for organic materials of types II and III.

In the Blake-Bahama Formation, T_{max} ranges from 418 to 436°C with an average of about 426°C. The higher values could reflect a moderate inertinite content. The location of the formation above the oil window is in agreement with the present depth of burial (1300 to 1560 m). In the Hatteras Formation, the samples with TOC lower than 0.2 wt.% do not give reliable T_{max} data, so only two samples give reliable temperature data (430°C and 433°C). In the organic-matter-rich level at the top of the Hatteras Formation, T_{max} is much lower because the type of organic matter changes (average T_{max} = 416°C). The sample richer in TOC from the Plantagenet Formation (Sample 603B-29-1, 57–62 cm) gives a T_{max} of 440°C, which is probably due to reworked material.

Nature of the Organic Matter (Table 1, Fig. 2)

Three types of kerogen can be distinguished from pyrolysis studies. Types I and II are related to lacustrine or marine reducing environments and are derived mainly from planktonic organisms, whereas type III comes from organic matter derived from terrestrial plants and transported to a marine or nonmarine environment with a moderate level of degradation. Intermediate kerogens are common, particularly between types II and III. They result from a mixture of marine and terrestrially derived organic matter or from the biodegradation of marine organic matter (Tissot and Pelet, 1981). A fourth type of organic matter is residual organic matter, which may be either recycled from older sediments by erosion or deeply altered by subaerial weathering (Tissot et al., 1979).

In the Blake-Bahama Formation, two sets of organic matter can be distinguished. A deeply altered, residual organic matter occurs in the samples of Barremian or Hauterivian age (Samples 603B-53-4, 135–139 cm; 603B-66-2, 135–138 cm, and 603B-71-5, 125–130 cm) and at the bottom of the hole in Sample 603B-81-3, 124–129 cm, whereas in Cores 603B-75 and -76 the marls contain organic matter of terrestrial origin (Fig. 2).

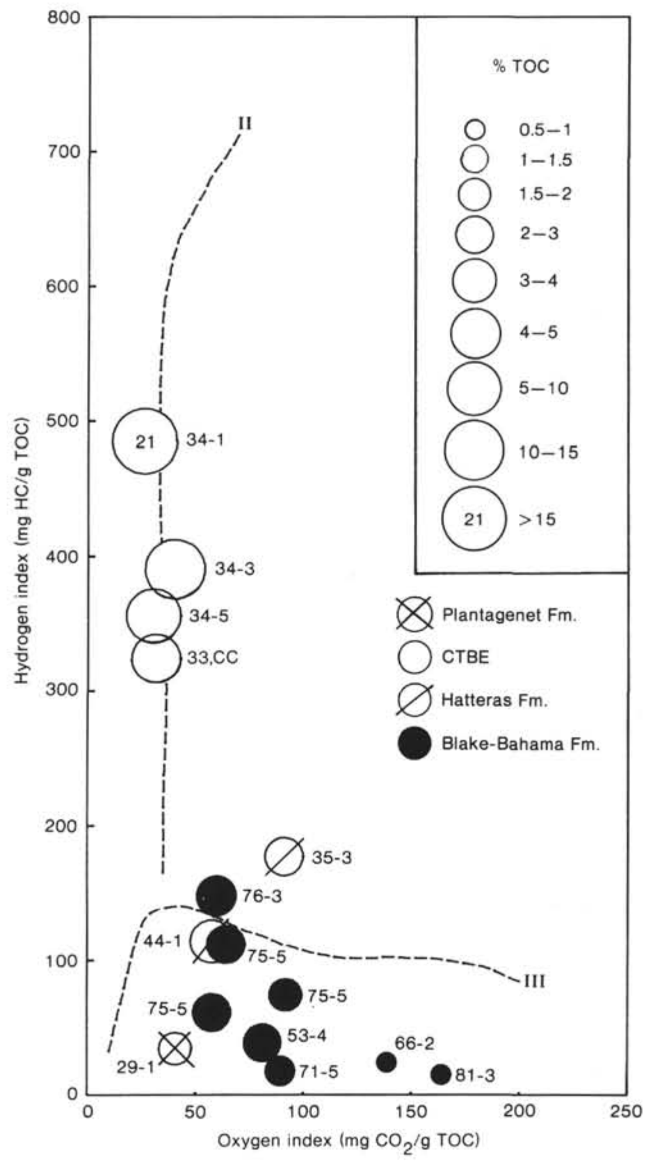

Figure 2. Characterization of the organic matter in Hole 603B by pyrolysis method. Size of the circles is proportional to total organic carbon. CTBE = Cenomanian/Turonian Boundary Event. Samples identified by Core-Section number.

In the Hatteras Formation, the dark claystones (with an average TOC content of 3 wt.%) contain type III organic matter. This terrestrial organic matter is common to the entire "Black Shales Formation" wherever the sites may be (105, Leg 11; 391, Leg 44; or 534, Leg 76, Herbin et al., 1983). On the other hand, the high TOC content at the top of the Hatteras Formation (Cores 603B-34 and -33) belongs chiefly to a type II organic matter with a hydrogen index (HI) ranging from 324 to 485 mg HC/g TOC. The preservation of organic matter of planktonic origin at this level indicates an anoxic environment which coincides with the Cenomanian/Turonian boundary.

Above the CTBE, the organic matter is residual (Sample 603B-29-1, 57–62 cm) in the Plantagenet Formation.

Kerogen Study (Table 1, Fig. 3)

Eleven samples were selected from different formations at Site 603 and prepared for elemental analysis of the kerogen concentrations (Table 1). The H/C and O/C ratios in Table 1 are plotted on a Van Krevelen diagram (Fig. 3) according to the three reference evolution paths for types I, II, and III kerogens from ancient sediments (Tissot et al., 1974).

An immature stage can be assigned to all samples. Samples 603B-71-5, 125–130 cm, of Hauterivian age, and 603B-29-1, 57–62 cm, of Santonian age, are located below the limit for kerogen of types I, II or III. They contain degraded kerogen considered as residual organic material (Tissot et al., 1979). A group of five samples is located near the evolution path for type III; Samples 603B-75-5, 17–19 cm, of Valanginian age, and 603B-35-3, 74–76 cm, of Cenomanian age, have a higher H/C atomic ratio than Samples 603B-81-3, 124–129 cm (Valanginian), 603B-66-2, 135–138 cm (Hauterivian), and 603B-44-1, 23–24 cm (Aptian). From pyrolysis analysis, Samples 603B-81-3, 124–129 cm and 603B-66-2, 135–138 cm were previously interpreted as consisting of residual organic matter, but the kerogen study indicates a type III

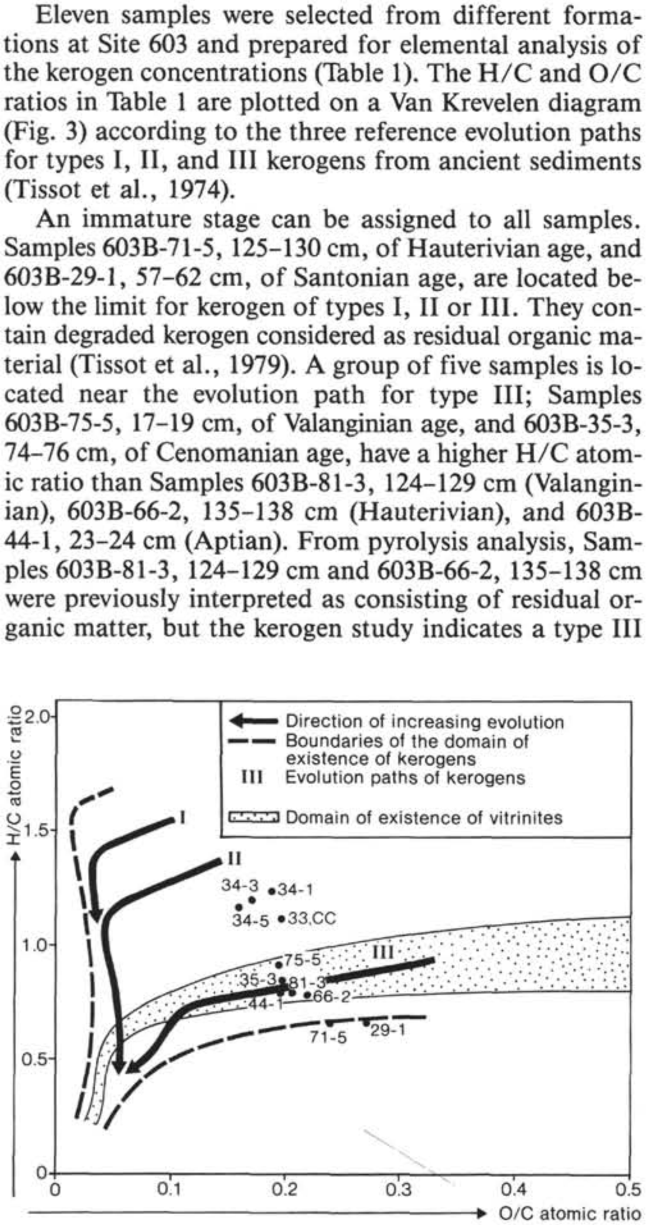

Figure 3. Elemental analysis of the kerogen: H/C and O/C diagram. Hole 603B samples identified by Core-Section number.

origin. All samples from Cores 603B-34 and -33 are located between types II and III, with H/C ranging between 1.11 and 1.23. The sample analyzed in the CTBE at Site 105 (Samples 105-9-4, 13–15 cm) with H/C = 1.10 and O/C = 0.19 fits well with these samples from Site 603. All these data indicate the presence of some type II organic matter with a planktonic origin at the top of the Hatteras Formation. This preservation is quite specific to the CTBE and does not occur in either the older or the younger sediments. The CTBE appears to be the most favorable period for sedimentation of type II organic matter, whereas in the other claystones only type III accumulated.

Chloroform Extraction Study (Table 1, Fig. 4)

The extracts collected from 13 selected samples (Table 1) represent 0.016–0.387 wt.% of rock, corresponding to 1.1–3.1 wt.% of extract to TOC. As is usually found in DSDP sites, polar compounds with high molecular weight predominate in the extract. Thus the hydrocarbons are represented by 5.7–15.3 wt.% of the total extract (exceptionally, 32.2 in Sample 603B-29-1, 57–62 cm).

Ten extracts were then selected for capillary gas chromatography (GC) studies (Fig. 4). The GC analysis of saturates + unsaturates reveals comparable chromatograms for the samples analyzed from the Valanginian (Sample 603B-75-5, 17–19 cm), Hauterivian (Sample 603B-71-5, 125–130 cm), Barremian (Sample 603B-53-4, 135–139 cm), Aptian (Sample 603B-44-1, 23–24 cm), Cenomanian (Sample 603B-35-3, 74–76 cm), and Santonian (Sample 603B-29-1, 57–62 cm). Predominance of odd-numbered molecules in the n-C_{23} to n-C_{35} fraction indicates immature material. Pristane slightly predominates over phytane in all these samples. The geological environment can influence the formation of the isoprenoids issuing from phytol after deposition or during maturation (Sever and Parker, 1969; Simoneit, 1973; Ikan et al., 1975a, b). The sediments where pristane is equal to or higher than phytane should indicate an environment unfavorable to the preservation of organic matter. The degradation of phytol indicates the phytenic acid precursor of pristene and then of pristane. In contrast, in Samples 603B-34-5, 23–25 cm and 603B-34-1, 82–83 cm from the Cenomanian/Turonian boundary—much richer in TOC (4.6–20.4 wt.%)—the GC study shows that phytane predominates over pristane. This richness in isoprenoids, particularly in phytane, could indicate deposition in a more restricted environment. The occurrence of organic matter of marine origin is, furthermore, suggested by the presence of sterane/sterene, triterpane/triterpene molecules in the n-C_{27}+ range (Roucaché et al., 1979) (Fig. 4).

THE CENOMANIAN/TURONIAN BOUNDARY EVENT

Site 105

Site 105 was drilled during Leg 11 on the lower continental rise hills off Cape Hatteras (Ewing and Hollister, 1972). In Sections 105-9-3 and 105-9-4 (289 to 292 m), a major lithological change marks the top of the "black

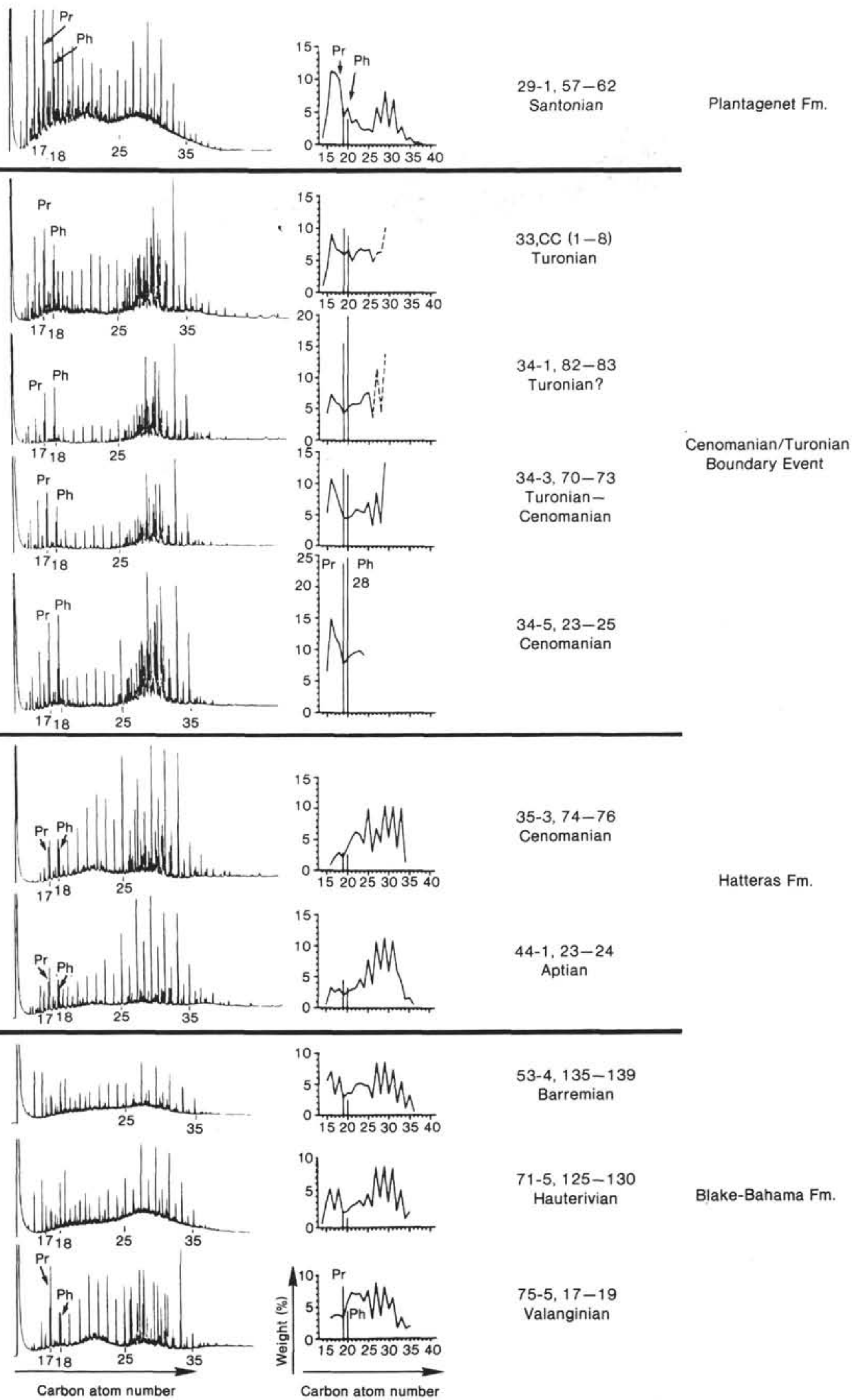

Figure 4. Chromatogram of the saturated + unsaturated fraction of samples from Hole 603B, Gas chromatography analysis on quartz col. capil. CP SIL5 (θ int: 0.5 mm, L = 25 m), injected 0.2 μl splitless (model Varian 3700). Pr = pristane, Ph = phytane.

shales" sedimentation of the Hatteras Formation. Above this break, the Upper Cretaceous to lower Tertiary multicolored claystones (from the top of Core 105-9 to Core 105-5) show a very low sedimentation rate, resulting from the small proportion of terrigenous material and the absence of calcareous and siliceous microfossils. In this interval, the major components of the sediments are of volcanic origin, with metal enrichments. This volcanic activity can be correlated to a major phase in the tectonic history of the North Atlantic Ocean (Lancelot et al., 1972). Below the break (from the bottom of Core 105-9 to Core 105-17, the black and olive green clays of Cenomanian to Albian age are interpreted as reflecting the alternation of reducing and mildly oxidizing conditions. The TOC of the black clays in Cores 17 to 10 range between 1 and 5 wt.%, and higher TOC is reached in Core 9: up to 10 in Sections 105-9-5 to 105-9-6 and even up to 25 in Sections 105-9-3 to 105-9-4 (Herbin and Deroo, 1982). These high contents, located just within the break, underlie the stratigraphic "hiatus" between upper Cenomanian and Senonian, at a time when the accumulation rate should have been < 1 m/Ma. New results obtained from the stratigraphic synthesis of the DSDP sites in the North Atlantic (Müller et al., 1983) have made it possible to date Section 5 at 93 cm as late Cenomanian with Sections 3 and 4 being located in the CTBE.

A detailed sampling along a 7.5-m interval between 287.5 and 295 m (Core 105-9 from Sections 2 to 6), allows study of the TOC content and the type of organic matter in this condensed sedimentary section. A typical alternation of black and green claystones occurs from the bottom of Section 6 to Section 4 at 87 cm. As in the whole Hatteras Formation, the thickness of the green layers is much greater than the black ones. In contrast, from Section 4 at 86 cm to Section 3 at 110 cm, the lithology is composed of about 20 sequences of black claystones with cm-scale to mm-scale green layers (see description in Fig. 5). The TOC is very high in this interval: 10 to 25 wt.% (Table 2) in contrast to the general content of the Hatteras Formation (2 to 5) (Fig. 6). All the interbedded green claystones have low TOC (0.35) like the moderate brown claystones of the top of the core from Section 3 at 110 cm to Section 1. In all the facies the carbonate contents are very low (0 to 17 wt.% $CaCO_3$).

The organic matter is mainly detrital in the lower part of Core 105-9 (Sections 5 and 6) as it was below, in the Hatteras Formation. In the break from Sample 105-9-4, 86 cm to 105-9-3, 110 cm, the organic matter is a mixture of types II and III (Fig. 6). This composition is confirmed by the elemental analysis of the kerogen in Sample 105-9-4, 13–15 cm ($H/C = 1.10$ and $O/C = 0.19$).

At 95 Ma, Site 105 was located in an abyssal paleoenvironment; paleodepth reconstruction indicates a depth of approximately 4100 m (Chénet and Francheteau, 1979).

Site 603

Since preparation of the kerogen concentrates (Huc et al., 1978) was the same for both the geochemical study (elemental analysis) and the palynological study, both analyses were performed on the samples issued from the Organic Geochemistry Panel in order to obtain information about the age of the sediments from the marine palynomorphs, especially dinoflagellate cysts.

Three samples from Core 34, Sample 603-33,CC, and one sample from Core 29 were analyzed. Fifty-five species were recovered (Fig. 7). Dinocysts from Core 34 are poorly preserved, in contrast to the well-preserved specimens from Core 29. Comparison with well-known stratigraphic ranges established in accurately dated European, Canadian, and African onshore sections and local ranges established at previous DSDP sites in the North Atlantic, especially Site 105, made it possible to determine the age of these samples.

1. *Sample 603B-34-5, 23–25 cm*: Latest Albian (Vraconian) to early Cenomanian. The stratigraphically significant species are listed:

Epelidosphaeridia spinosa (Plate 1, Fig. 1) first appears in the Vraconian of the Col de Palluel section (Davey and Verdier, 1973).

Litosphaeridium siphonophorum (Plate 1, Fig. 2) first occurs in the late Albian of France (Davey and Verdier, 1973) and of Morocco (Below, 1982).

Odontochitina costata (Plate 1, Fig. 3) and *Ovoidinium verrucosum* first occur in the Vraconian (Davey and Verdier, 1973).

The assemblage is characterized by a high percentage of *Cyclonephelium hughesii* (Plate 1, Fig. 8), and *Ovoidinium ovale* (Plate 1, Fig. 4). *E. spinosa* and *L. siphonophorum* first appear at or near the base of the *Spinidinium echinoideum* zone of Habib, 1977, in Holes 105 (Habib, 1972) and 534A (Habib and Drugg, 1983).

2. *Sample 603B-34-3, 70–73 cm*: Cenomanian. The species are considered to be stratigraphically important are listed:

Palaeohystrichophora infusorioides (Plate 1, Fig. 9) first appears in the Vraconian (Davey and Verdier, 1973).

Dinogymnium acuminatum (Plate 1, Fig. 7). The first occurrence of *Dinogymnium* species is in the upper part of the Turonian from the Turonian stratotype area (Foucher, 1982). One specimen has been recorded in the Cenomanian from the southwest of France (Azéma et al., 1981). The genus has been recorded sporadically from the middle Cenomanian of Africa (Boltenhagen, 1977). According to Morgan (1978), S. Jardiné has found these *Dinogymnium* species in African sediments older than Santonian. Species of *Dinogymnium* have not been recorded from the lower Cenomanian of Morocco (Below, 1981, 1982). Thus a middle or late Cenomanian through Turonian age is suggested by dinocysts. *Dinogymnium* species has been recorded in Sample 398D-56-2, 122–124 cm (Masure, 1984). Futher, the genus *Dinogymnium* has been observed in Sample 101A-4-1, 136–139 cm and Section 105-10-2 (Habib, 1972; Habib and Knapp, 1982); these samples are dated Vraconian or early Cenomanian by foraminifers and radiolarians (Müller et al., 1983).

3. *Sample 603B-34-1, 82–83 cm*. Dinocysts are very rare and poorly preserved against a background of abundant organic matter.

Cyclonephelium vannophorum is recovered in this sample. It first occurs in the European Cenomanian (Davey, 1969).

4. *Sample 603B-33,CC, (01-08 cm)*: upper Cenomanian–lower Turonian. For this sample a few diagnostic species have been recorded.

Trithyrodinium suspectum (Plate 1, Fig. 13) first appears in the Cenomanian (Manum and Cookson, 1964).

T. suspectum has been recovered in Sample 105-9-5, 88–89 cm (Habib and Knapp, 1982). A late Cenomanian–lower Turonian age is suggested by radiolarians (Müller et al., 1983).

Florentinia resex (Plate 1, Fig. 11) has been recorded in the European Turonian (Davey and Verdier, 1976) and also from the Aptian and Albian of Morroco (Below, 1982).

Litosphaeridium siphonophorum is present in this sample. It last occurs in the upper part of the Cenomanian (Foucher, 1979, 1982).

5. *Sample 603B-29-1, 57–62 cm*: Santonian. A rich and diverse microplankton assemblage was recovered from this sample. The stratigraphically significant species are:

Senoniasphaera rotundata (Plate 2, Fig. 1) and *S. protrusa* (Plate 2, Fig. 2). *S. rotundata* appears in the lower part of the Turonian stratotype (Foucher, 1982) and in the Coniacian of Canada (Bujak and Williams, 1978). *S. protusa* appears in the middle Santonian of France (Foucher, 1979) and in the Turonian of Canada (Bujak and Williams, 1978).

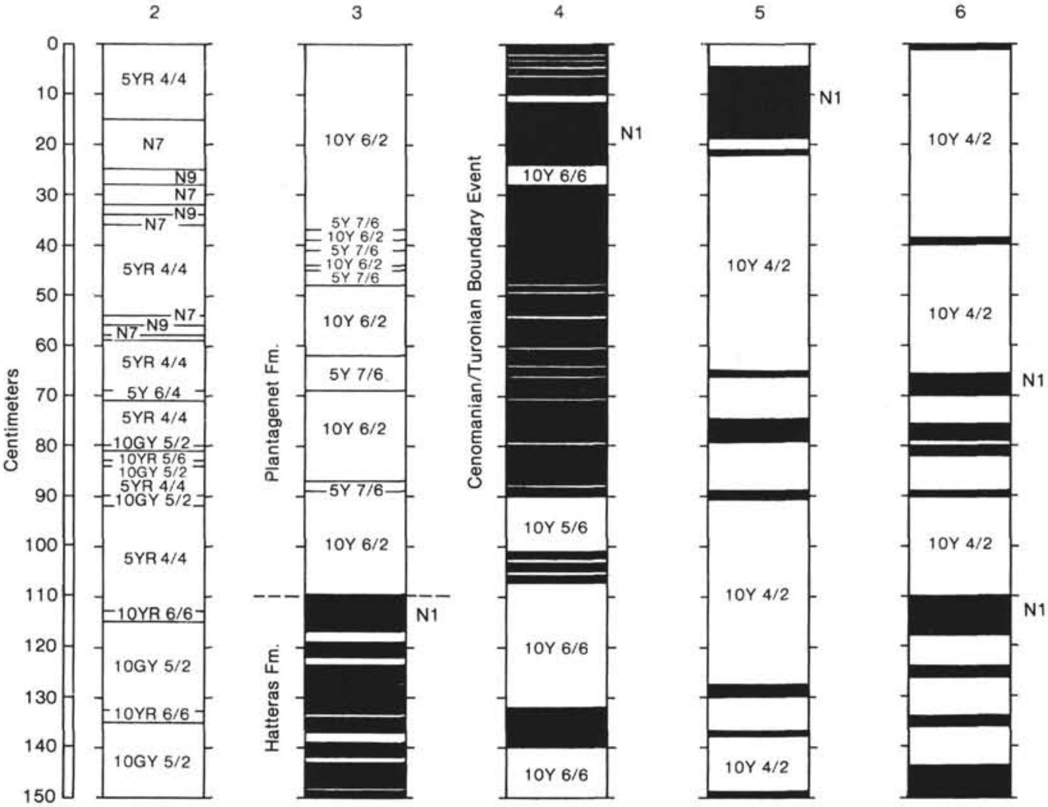

Figure 5.Lithological description of Sections 105-9-2 to 105-9-6 (Cenomanian/Turonian Boundary Event). Standard color coding noted on column.

Dinogymnium euclaense and *Coronifera striolata* (Plate 2, Fig. 5) first occur in the Santonian of Canada (Bujak and Williams, 1978).

After the CTBE was recognized from the enrichment in type II organic matter in the samples issued from the Organic Geochemistry Panel and that recognition confirmed by the ages just given the break between the Hatteras and Plantagenet Formations (Core 603B-34) was sampled specifically for a detailed study of the organic content and nature of the organic matter along the CTBE. This study shows the advent of the anoxic environment during the CTBE and the cyclic influences of anoxia, more and more favorable to the preservation of marine organic matter, from the bottom to the top of Core 603B-34 (i.e., between 1136.5 and 1127.5 m).

In Core 34, 19 sedimentary sequences were determined on the basis of the sedimentological descriptions (Fig. 8) and results on geochemical data (Fig. 9). These sequences are named Sequences A to S and may be subdivided into two or more subunits, one labeled by odd numbers (A1, A3, B1, C1, etc.) corresponding to the dusty yellow-green 5GY 5/2 claystones with greyish yellow green laminations 5GY 7/2, and one labeled by even numbers (A2, A4, B2, C2, etc.), corresponding to the laminated black claystones. In the following description we study the sequences stratigraphically, from the bottom of Core 603B-35 to the top of Core 603B-34. The sequences are devoid of any variations in the carbonate content (Fig. 9). Whatever the lithology (green or dark claystones), the $CaCO_3$ content is less than 10 wt.% with an average content of 5, except in Sample 603B-34-3, 118–119 cm, where it reaches 21 (Table 3).

In Core 603B-35 the alternations of black shales from the Hatteras Formation contain mainly type III organic matter (see the detailed study of Sample 603B-35-3, 74–76 cm). The petroleum potential is medium to good (2.15 to 8.36 kg (HC/t of rock) in the richer sample, where the hydrogen indices range from 105 to 217 mg HC/g TOC. At the bottom of Core 603B-34, the green claystones A1 of sequence A) are very poor in TOC (<0.2 wt.%). The sequence is bimodal, with two slight enrichments in TOC: 0.7 wt.% in A2 and 1.04 to 1.79 wt.% in A4; both contain an organic matter of type III origin. The sequences above B, C, and D, have very thin, dark levels (B2 = 2 cm, C2 = 4 cm, D2 = 8 cm), but they are richer in TOC (2.06 to 5.29 wt.%), with a petroleum potential ranging from 3.6 to 18.1 kg HC/t of rock. The hydrogen indices are often higher than 300 and even reach 354 mg HC/g TOC in Sample 603B-34-5, 82–83 cm, indicating a greater ratio of marine organic matter and/or less degradation than in the underlying dark claystones. This pattern extends to sequences E and F, where the dark claystones are again thicker (E2 = 36 cm, F2 = 54 cm). The TOC contents reach 7.7–7.8 wt.% at the top of the sequences, corresponding to a petroleum potential near 30 kg HC/t of rock. The hydrogen indices are also a slightly higher, about 380 mg HC/g TOC. Sequence G is different because of the bioturbated levels (G3 and G5) on both sides of dark claystones (G4), where

Table 2. Carbonate, organic carbon, and pyrolysis data in the Cenomanian/Turonian Boundary Event, Sections 105-9-2 to 105-9-6.

	Core-Section (level in cm)	Sub-bottom depth (m)	Mineral carbon (%)	$CaCO_3$ (%)	TOC (%)	$S_1 + S_2$ (kg HC/t rock)	HI	OI	T_{max}
	9-2, 23	287.73	0.63	5	0.35	3.74			
	9-2, 58	288.08	1.32	11	0.24	2.37			
	9-2, 100	288.50	1.26	10	0.19	2.27			
	9-2, 115	288.65	1.50	12	0.22	2.66			
	9-2, 140	288.90	1.20	10	0.19	2.23			
Plantagenet Fm.	9-3, 24	289.24	1.35	11	0.22	2.31			
	9-3, 44	289.44	0.68	6	0.16	0.04			
	9-3, 57	289.57	1.44	12	0.16	1.86			
	9-3, 67	289.67	1.80	15	0.22	2.48			
	9-3, 94	289.94	1.50	12	0.15	1.70			
	9-3, 109	290.09	0.87	7	0.14	1.16			
	9-3, 100	290.10	2.52	21	1.32	1.54	89	153	411
	9-3, 111	290.11	1.50	12	4.40	5.18	104	90	417
	9-3, 112	290.12	0.00	0	5.59	6.61	117	98	410
	9-3, 113	290.13	1.74	14	10.31	24.94	225	62	412
	9-3, 114	290.14	1.20	10	7.69	11.70	140	74	410
	9-3, 118	290.18	0.96	8	0.72	0.88	107	133	407
	9-3, 120	290.20	1.11	9	3.64	8.14	204	71	410
	9-3, 121	290.21	2.46	20	9.83	35.35	327	71	411
	9-3, 122	290.22	2.22	18	6.91	22.30	292	78	413
	9-3, 123	290.23	1.38	11	0.27	1.02			
	9-3, 125	290.25	1.74	14	15.20	54.67	330	58	411
	9-3, 126	290.26	1.68	14	12.58	45.55	331	68	412
	9-3, 128	290.28	0.96	8	12.68	43.85	312	66	410
	9-3, 132	290.32	1.50	12	15.49	59.80	353	63	409
	9-3, 134	290.34	1.20	10	0.22	0.86			
	9-3, 135	290.35	1.56	13	12.52	42.25	309	56	412
	9-3, 138	290.38	0.00	0	0.15	1.27			
	9-3, 139	290.39	0.00	0	11.61	42.70	335	66	410
	9-3, 145	290.45	0.12	1	12.61	50.55	364	77	410
	9-3, 147	290.47	0.04	0	17.10	59.99	340	51	405
	9-3, 149	290.49	0.27	2	0.27	1.15			
	9-3, 150	290.50	1.08	9	7.87	27.15	309	84	413
	9-4, 2	290.52	0.78	6	12.78	45.25	323	67	411
	9-4, 7	290.57	1.20	10	21.07	81.50	348	56	408
	9-4, 10	290.60	1.50	12	8.28	24.15	264	74	411
	9-4, 11	290.61	0.87	7	0.27	1.23			
	9-4, 11	290.61	0.12	1	0.32	0.09			
	9-4, 12	290.62	1.98	16	7.09	21.10	265	69	414
	9-4, 13	290.63	0.04	0	9.70	38.73	399	28	412
	9-4, 16	290.66	2.04	17	9.55	36.20	343	69	412
	9-4, 23	290.73	1.68	14	13.30	49.70	340	66	410
Cenomanian/Turonian Boundary Event	9-4, 25	290.75	0.96	8	0.11	0.87			
	9-4, 25	290.78	1.11	9	0.37	0.91	219	270	417
	9-4, 29	290.79	1.80	15	6.11	18.60	281	78	416
	9-4, 36	290.86	1.56	13	6.48	24.15	337	91	412
	9-4, 39	290.89	1.92	16	4.88	11.55	210	68	416
	9-4, 43	290.93	1.44	12	10.18	29.45	259	64	410
	9-4, 52	291.02	1.50	12	4.81	9.80	174	80	415
	9-4, 53	291.03	0.78	6	0.17	0.70			
	9-4, 58	291.08	1.26	10	9.37	28.15	274	67	413
	9-4, 62	291.12	1.26	10	13.78	48.65	321	56	411
	9-4, 69	291.19	1.98	16	4.64	11.15	213	79	414
	9-4, 70	291.20	0.84	7	0.29	0.64			
	9-4, 73	291.23	0.00	0	13.92	49.80	329	60	410
	9-4, 79	291.29	0.00	0	1.26	1.07	66	198	404
	9-4, 80	291.30	0.24	2	14.62	54.25	342	66	411
	9-4, 82	291.32	0.00	0	23.80	74.13	301	52	398
	9-4, 83	291.33	0.30	2	9.18	37.65	373	97	409
	9-4, 86	291.36	0.72	6	11.96	36.75	280	69	410
	9-4, 87	291.37	0.42	3	0.16	0.96			
	9-4, 88	291.38	0.36	3	2.38	5.86	214	89	413
	9-4, 89	291.39	0.54	4	0.18	1.04			
	9-4, 93	291.43	0.54	4	0.07	0.80			
	9-4, 103	291.53	0.84	7	2.75	4.92	158	98	412
	9-4, 106	291.56	0.51	4	0.10	0.88			
	9-4, 113	291.63	0.51	4	0.15	0.91			
	9-4, 118	291.68	0.78	6	0.09	0.81			
	9-4, 120	291.70	0.76	6	0.27	0.26			
	9-4, 131	291.81	1.02	8	0.14	0.83			
	9-4, 132	291.82	1.74	14	6.57	19.50	275	84	418
	9-4, 138	291.88	1.32	11	6.67	16.15	217	90	412
	9-4, 141	291.91	1.44	12	3.93	9.05	202	73	419
	9-4, 142	291.92	0.87	7	0.42	0.75	155	269	419
	9-4, 148	291.98	1.02	8	0.14	0.79			

Table 2 (continued).

	Core-Section (level in cm)	Sub-bottom depth (m)	Mineral carbon (%)	$CaCO_3$ (%)	TOC (%)	$S_1 + S_2$ (kg HC/t rock)	HI	OI	T_{max}
	9-5, 4	292.04	0.90	7	0.11	0.87			
	9-5, 5	292.05	1.74	14	8.24	25.45	284	68	417
	9-5, 7	292.07	1.26	10	10.21	25.90	230	58	416
	9-5, 14	292.14	2.22	18	6.56	14.60	197	63	415
	9-5, 18	292.18	1.74	14	4.64	9.36	183	65	413
	9-5, 21	292.21	0.90	7	0.21	1.41			
	9-5, 22	292.22	1.92	16	3.52	5.66	145	56	419
	9-5, 23	292.23	0.96	8	0.42	1.29	226	126	387
	9-5, 46	292.46	1.08	9	0.11	0.91			
	9-5, 65	292.65	1.14	9	0.13	1.07			
	9-5, 66	292.66	1.80	15	3.40	7.45	193	49	433
	9-5, 67	292.67	1.26	10	0.20	0.84			
	9-5, 75	292.75	1.92	16	2.62	3.95	126	46	429
	9-5, 79	292.79	2.04	17	1.72	3.02	158	80	425
	9-5, 80	292.80	1.11	9	0.50	0.76	134	60	442
	9-5, 89	292.89	2.16	18	3.22	5.12	133	50	426
	9-5, 93	292.93	1.04	9	4.29	6.94	158	65	419
	9-5, 94	292.94	1.26	10	0.13	0.67			
	9-5, 119	293.19	0.66	5	0.16	1.46			
	9-5, 127	293.27	0.78	6	0.18	1.29			
	9-5, 128	293.28	1.08	9	4.54	7.55	142	50	425
	9-5, 130	293.30	1.20	10	3.24	5.05	134	45	427
	9-5, 132	293.32	0.87	7	0.24	1.33			
	9-5, 134	293.34	0.72	6	3.12	3.75	117	66	428
	9-5, 137	293.37	1.02	8	0.72	1.35	150	64	436
	9-5, 138	293.38	0.75	6	0.41	1.16	232	95	424
Hatteras Fm.	9-5, 144	293.44	0.87	7	0.18	0.99			
	9-5, 150	293.50	0.90	7	1.01	1.24	103	51	500
	9-6, 1	293.51	1.08	9	0.78	2.78	(324)	(49)	(589)
	9-6, 3	293.53	0.96	8	0.31	2.23			
	9-6, 39	293.89	1.08	9	0.28	1.69			
	9-6, 40	293.90	1.56	13	4.14	5.90	121	47	431
	9-6, 41	293.91	1.02	8	0.25	1.67			
	9-6, 64	294.14	1.08	9	0.14	1.20			
	9-6, 69	294.19	1.50	12	8.58	18.30	192	57	418
	9-6, 75	294.25	1.11	9	0.24	1.62			
	9-6, 78	294.28	0.87	7	2.51	3.00	84	50	407
	9-6, 82	294.32	1.32	11	9.47	16.20	156	53	417
	9-6, 87	294.37	0.87	7	0.19	1.11			
	9-6, 90	294.40	0.60	5	4.78	6.25	108	54	422
	9-6, 91	294.41	0.63	5	0.18	1.29			
	9-6, 106	294.56	0.72	6	0.16	1.02			
	9-6, 111	294.61	0.40	3	4.03	3.13	73	83	413
	9-6, 114	294.64	0.72	6	7.29	12.30	152	49	417
	9-6, 116	294.66	0.54	4	7.42	12.40	150	48	417
	9-6, 117	294.67	0.60	5	7.36	11.55	138	49	417
	9-6, 122	294.72	0.42	3	0.16	1.00			
	9-6, 125	294.75	0.36	3	7.03	9.92	130	62	417
	9-6, 130	294.80	0.60	5	0.23	0.98			
	9-6, 135	294.85	0.48	4	6.33	7.02	100	59	418
	9-6, 141	294.91	0.63	5	0.23	1.02			
	9-6, 144	294.94	0.92	8	1.60	1.78	84	78	407
	9-6, 150	295.00	0.78	6	1.79	1.90	83	76	416

Note: Parentheses indicate doubtful data.

the TOC content is often lower than 1 wt.% and the hydrogen indices lower than 50 mg HC/g TOC. Because of the bioturbated area, the trend of sequence G is symmetrical, and the highest TOC content is reached in the middle of G4 (Samples 603B-34-4; 56–57 cm: TOC = 6.5 wt.%, $S_1 + S_2$ = 26.54 kg HC/t of rock, and HI = 390 mg HC/g TOC). In sequences H and K (sequences I and J being undeveloped), the TOC contents increase again: 9.12 wt.% in H2 (Sample 603B-34-3, 148–149 cm) and 11.45 wt.% in K2 (Sample 603B-34-3, 88–89 cm), corresponding respectively to petroleum potentials of 39.13 and 52.90 kg HC/t of rock and hydrogen indices of 404 and 442 mg HC/g TOC. The thicker sequences of black shales in Core 34 correspond to sequences L to R, where the green claystones are often very reduced. In sequences L to O the TOC content increases to 14 wt.%, corresponding to a petroleum potential of 68 kg HC/t of rock and to hydrogen indices close to 500 mg (HC/g TOC. The highest geochemical results are obtained in sequences P and Q, that is, in Sample 603B-34-1, 124–125 cm (P2): TOC = 17.98 wt.%, $S_1 + S_2$ = 96.05 kg HC/t of rock, and HI = 507 mg HC/g TOC in Sample 603B-34-1, 82–83 cm (Q2), TOC = 20.40 wt.%, and $S_1 + S_2$ = 104.30 kg HC/t of rock. The highest hydrogen index belongs to Sample 603B-34-1, 90–91 cm, with HI = 525 mg HC/g TOC (Fig. 9, Table 3). In overlying sequences R and S, the enrichment decreases, since in R2 the TOC content is about 14.26 wt.%, $S_1 + S_2$ =

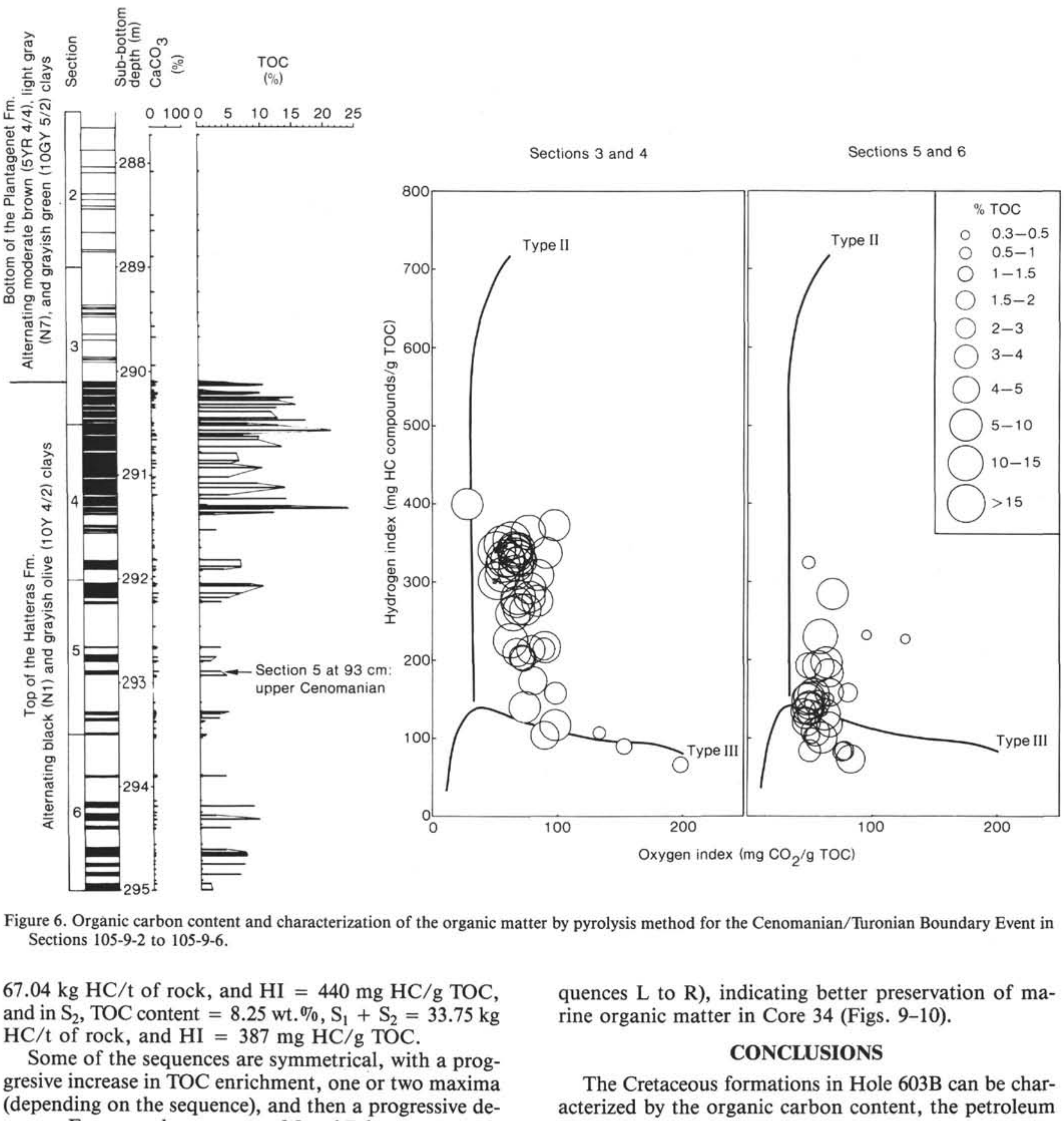

Figure 6. Organic carbon content and characterization of the organic matter by pyrolysis method for the Cenomanian/Turonian Boundary Event in Sections 105-9-2 to 105-9-6.

67.04 kg HC/t of rock, and HI = 440 mg HC/g TOC, and in S_2, TOC content = 8.25 wt.%, $S_1 + S_2$ = 33.75 kg HC/t of rock, and HI = 387 mg HC/g TOC.

Some of the sequences are symmetrical, with a proggresive increase in TOC enrichment, one or two maxima (depending on the sequence), and then a progressive decrease. For example, sequences M and R have one maximum, whereas sequences L and N have two (Fig. 9). Other sequences show an asymmetric variation of the TOC with a progressive increase but a sharp passage toward the green claystone of the following sequence. For example, the transition between sequences H and I occurs over 2 cm, with a decrease from 8.88 wt.% (Sample 603B-34-3, 138–139 cm) to 0.06 wt.% (Sample 603B-34-3, 136–137 cm) (Table 2). Such sharp transitions characterize the top of various sequences (E, F, H, L) (Fig. 9). The hydrogen indices fluctuate in the same way, with one or two maxima often higher than 400 mg HC/g TOC (sequences L to R), indicating better preservation of marine organic matter in Core 34 (Figs. 9–10).

CONCLUSIONS

The Cretaceous formations in Hole 603B can be characterized by the organic carbon content, the petroleum potential, and the type of organic matter.

In the Blake-Bahama Formation the samples richer in TOC (2.63 wt.%) have medium petroleum potential (4.35 kg HC/t of rock). The same content is reached in the black claystones of the Hatteras Formation, where the higher TOC content is about 3.43 wt.%, corresponding to medium petroleum potential (5.01 kg HC/t of rock). In these two formations the organic matter is type III and is quite immature (above the oil window).

The break between the Hatteras and Plantagenet formations (Core 34) corresponds to the Cenomanian/Turonian Boundary Event (CTBE), which is dated by di-

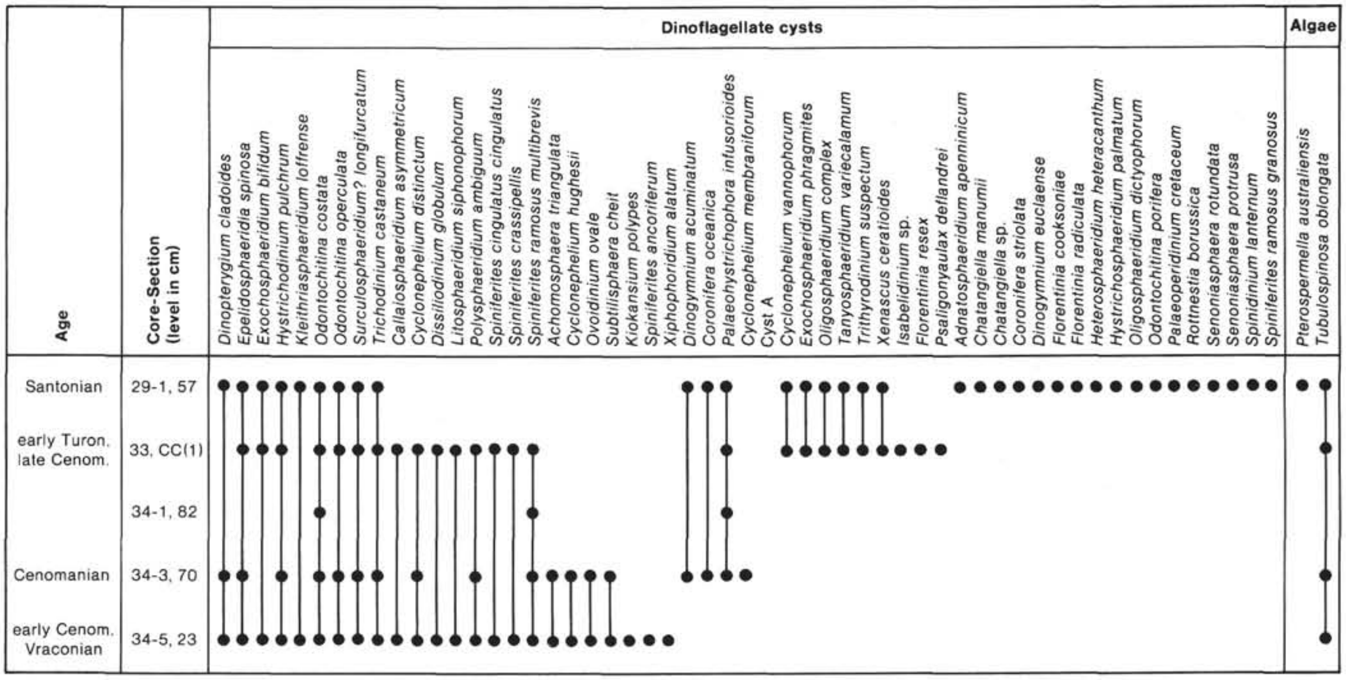

Figure 7. Stratigraphic distribution of selected dinoflagellate species in Hole 603B.

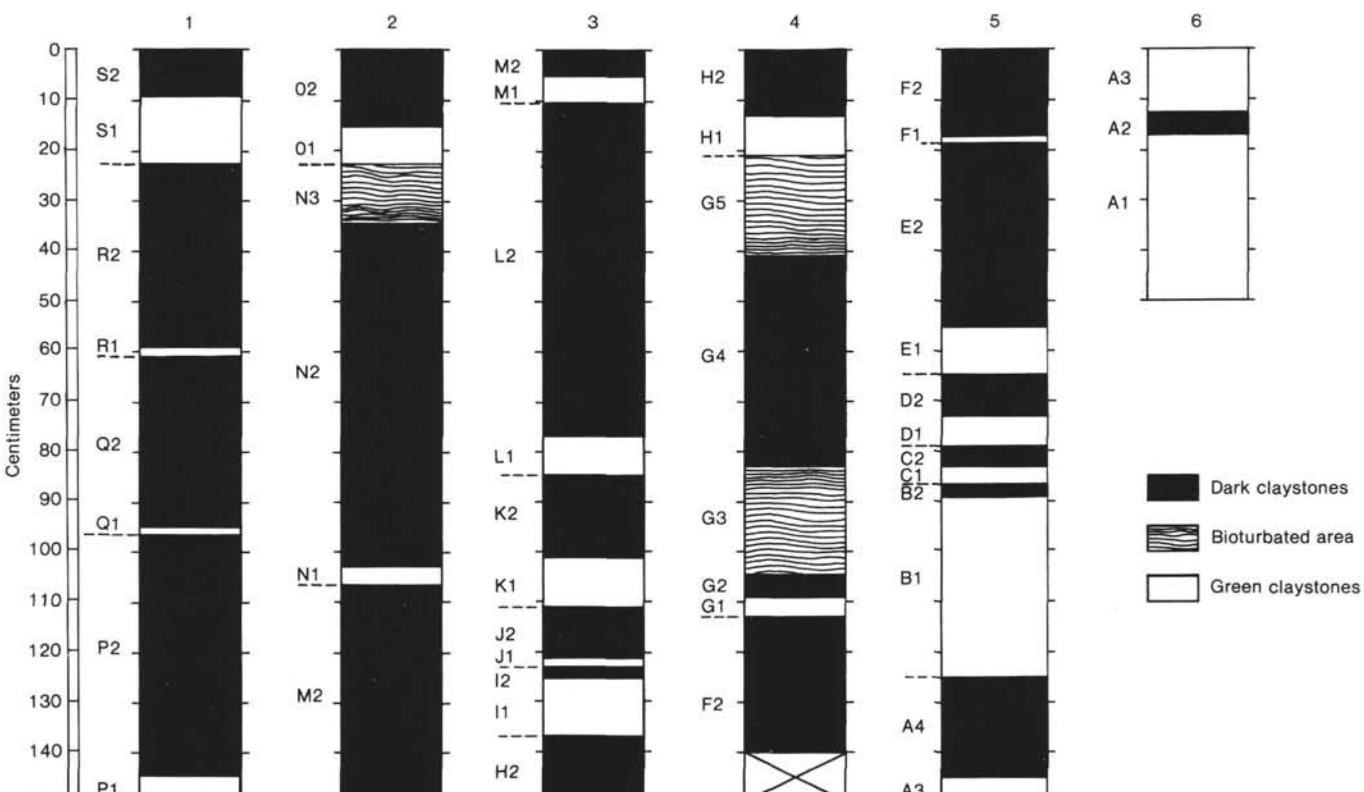

Figure 8. Lithological description of sequences A to S, corresponding to the Cenomanian/Turonian Boundary Event in Sections 603B-34-1 to 603B-34-6.

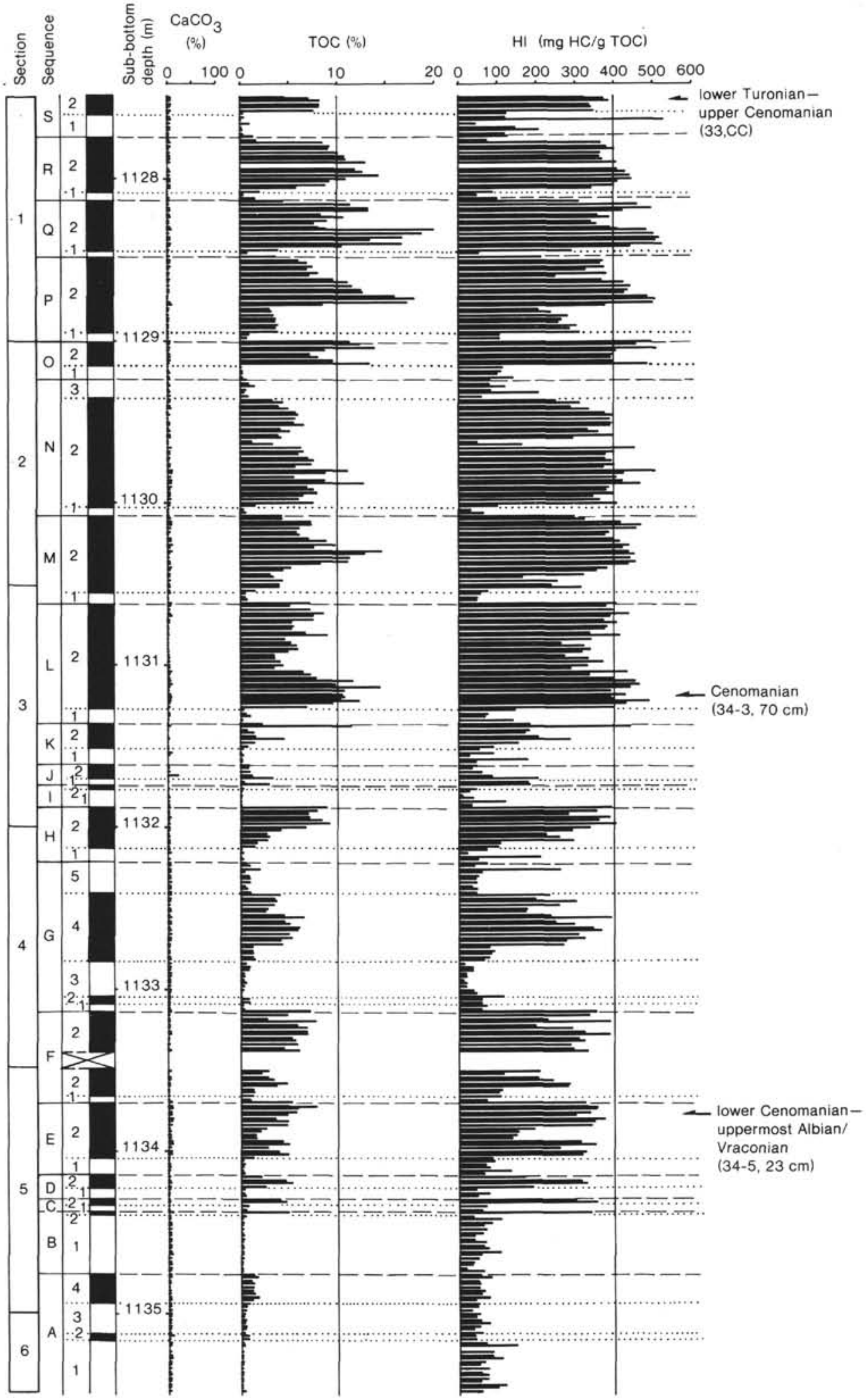

Figure 9. Vertical distribution of the organic carbon and carbonate content in the Cenomanian/Turonian Boundary Event at Site 603 (sequences A to S, Sections 603B-34-1 to 603B-34-6).

Table 3. Carbonate, organic carbon, and pyrolysis data in the Cenomanian/Turonian Boundary Event, Sample 603B-33,CC; Sections 603B-34-1 to 603B-34-6 and 603B-35-1 to 603B-35-4.

Sedimentary Sequence	Core-Section (level in cm)	Sub-bottom depth (m)	Mineral carbon (%)	$CaCO_3$ (%)	TOC (%)	$S_1 + S_2$	HI	OI	T_{max}
	33-0, 1	1127.49	0.66	5	4.58	15.27	324	31	420
	34-1, 0	1127.50	0.94	8	7.07	28.11	374	33	412
S2	34-1, 2	1127.52	0.78	6	8.25	33.75	387	37	411
	34-1, 4	1127.54	1.02	8	8.20	29.78	337	45	407
	34-1, 6	1127.56	0.62	5	8.13	30.05	342	52	409
	34-1, 8	1127.58	0.86	7	7.56	28.81	350	58	407
	34-1, 10	1127.60	0.47	4	0.34	0.51	(124)	(276)	(414)
	34-1, 12	1127.62	0.67	6	0.43	0.78	(121)	(195)	(406)
	34-1, 14	1127.64	0.95	8	0.14	0.88			
S1	34-1, 16	1127.66	0.71	6	1.01	0.58	45	73	418
	34-1, 18	1127.68	0.71	6	0.19	0.37	(147)	(232)	(432)
	34-1, 20	1127.70	0.63	5	0.28	0.73	(207)	(136)	(423)
	34-1, 22	1127.72	0.39	3	0.34	0.59	(121)	(91)	(408)
	34-1, 24	1127.74	0.27	2	1.36	1.97	126	60	410
	34-1, 26	1127.76	0.37	3	1.66	1.37	73	51	412
	34-1, 28	1127.78	0.78	6	8.54	33.26	367	32	409
	34-1, 30	1127.80	0.78	6	9.21	37.15	381	32	409
	34-1, 32	1127.82	0.46	4	9.08	38.75	402	27	410
	34-1, 34	1127.84	0.54	4	10.10	39.68	365	25	408
	34-1, 36	1127.86	0.62	5	10.77	42.39	364	22	406
	34-1, 38	1127.88	0.70	6	10.90	43.12	370	18	407
	34.1, 42	1127.90	0.38	3	12.91	56.25	406	23	406
R2	34-1, 40	1127.90	0.62	5	12.46	52.68	394	13	406
	34-1, 44	1127.94	0.38	3	11.84	51.59	409	24	405
	34-1, 46	1127.96	0.62	5	12.62	57.87	430	21	406
	34-1, 48	1127.98	0.54	4	14.26	67.04	440	17	405
	34-1, 50	1128.00	0.62	5	10.90	52.13	445	31	406
	34-1, 52	1128.02	0.62	5	9.20	40.39	410	34	405
	34-1, 54	1128.04	0.62	5	8.77	37.68	401	36	405
	34-1, 56	1128.06	0.67	6	5.78	30.95	342	38	408
	34-1, 58	1128.08	0.19	2	2.09	2.09	89	65	405
R1	34-1, 60	1128.10	0.15	1	0.37	0.27	49	141	427
	34-1, 62	1128.12	0.55	5	1.60	1.80	101	40	409
	34-1, 64	1128.14	0.43	4	4.49	14.69	310	29	413
	34-1, 66	1128.16	0.46	4	11.40	55.79	461	28	406
	34-1, 68	1128.18	0.70	6	13.24	70.31	496	30	407
	34-1, 70	1128.20	0.62	5	13.24	59.60	423	31	408
	34-1, 72	1128.22	0.54	4	8.34	33.20	359	46	408
	34-1, 74	1128.24	0.78	6	10.70	44.22	389	38	408
	34-1, 76	1128.26	0.38	3	8.98	30.74	340	36	409
	34-1, 79	1128.28	0.46	4	7.62	29.22	355	33	412
Q2	34-1, 80	1128.30	0.70	6	8.06	34.26	391	37	411
	34-1, 81	1128.31	0.46	4	8.83	39.06	410	39	411
	34-1, 82	1128.32	1.02	8	20.40	104.30	485	26	412
	34-1, 84	1128.34	0.46	4	18.72	99.90	503	36	410
	34-1, 86	1128.36	0.70	6	16.74	91.70	517	33	408
	34-1, 88	1128.38	0.62	5	13.38	72.40	506	37	408
	34-1, 90	1128.40	0.86	7	16.70	93.22	525	34	408
	34-1, 92	1128.42	0.54	4	10.47	49.32	442	41	409
	34-1, 94	1128.44	0.43	4	3.93	12.26	292	53	411
Q1	34-1, 96	1128.46	0.17	1	0.72	0.49	51	119	399
	34-1, 98	1128.48	0.55	5	3.69	8.35	214	35	413
	34-1, 100	1128.50	0.66	5	5.96	23.56	372	42	413
	34-1, 102	1128.52	0.54	4	6.90	26.58	364	45	411
	34-1, 104	1128.54	0.62	5	7.49	29.98	376	44	410
	34-1, 106	1128.56	0.30	2	6.88	24.02	326	55	413
	34-1, 108	1128.58	0.46	4	8.05	32.49	380	40	412
	34-1, 110	1128.60	0.30	2	7.11	18.82	248	58	410
	34-1, 112	1128.62	0.54	4	9.57	37.42	368	51	411
	34-1, 114	1128.64	0.30	2	11.07	49.59	424	49	411
	34-1, 116	1128.66	0.38	3	11.55	54.26	442	46	411
	34-1, 118	1128.68	0.38	3	12.50	57.69	436	41	412
P2	34-1, 120	1128.70	0.46	4	12.61	56.89	425	51	410
	34-1, 122	1128.72	0.14	1	15.91	81.52	486	48	409
	34-1, 124	1128.74	0.22	2	17.98	96.05	507	51	408
	34-1, 126	1128.76	0.78	6	17.23	90.55	500	53	409
	34-1, 128	1128.78	1.10	9	8.54	34.16	378	52	412
	34-1, 130	1128.80	0.43	4	3.07	6.80	205	108	413
	34-1, 132	1128.82	0.23	2	3.30	8.29	238	72	418
	34-1, 134	1128.84	0.27	2	3.47	10.26	282	68	414
	34-1, 136	1128.86	0.43	4	3.70	10.45	266	78	412
	34-1, 138	1128.88	0.31	3	3.63	9.96	257	42	409
	34-1, 140	1128.90	0.31	3	3.92	12.48	304	45	408
	34-1, 142	1128.92	0.35	3	3.70	11.38	287	53	410
	34-1, 144	1128.94	0.31	3	3.94	12.96	312	51	409

Table 3 (continued).

Sedimentary Sequence	Core-Section (level in cm)	Sub-bottom depth (m)	Mineral carbon (%)	$CaCO_3$ (%)	TOC (%)	$S_1 + S_2$	HI	OI	T_{max}
P1	34-1, 146	1128.96	0.27	2	0.93	1.24	105	113	410
	34-1, 148	1128.98	0.27	2	0.67	1.04	107	124	405
O2	34-2, 0	1129.00	0.62	5	11.27	58.76	497	38	411
	34-2, 2	1129.02	0.54	4	12.35	59.26	457	32	409
	34-2, 4	1129.04	0.54	4	13.86	74.25	509	49	409
	34-2, 6	1129.06	0.46	4	8.72	37.40	406	107	413
	34-2, 8	1129.08	0.54	4	7.16	30.93	399	98	414
	34-2, 10	1129.10	0.62	5	8.05	33.63	391	79	413
	34-2, 12	1129.12	0.62	5	9.56	40.59	398	28	412
	34-2, 14	1129.14	0.38	3	13.32	67.96	485	33	408
O1	34-2, 16	1129.16	0.15	1	0.15	0.25	(113)	(1113)	(443)
	34-2, 18	1129.18	0.27	2	0.21	0.33	(110)	(571)	(416)
	34-2, 20	1129.20	0.59	5	0.22	0.40	(100)	(559)	(450)
	34-2, 22	1129.22	0.43	4	0.22	0.46	(141)	(273)	(432)
N3	34-2, 24	1129.24	0.59	5	0.63	0.68	81	121	414
	34-2, 26	1129.26	0.31	3	0.90	0.86	79	100	419
	34-2, 28	1129.28	0.59	5	1.46	2.00	119	88	421
	34-2, 30	1129.30	0.35	3	0.58	0.64	83	155	412
	34-2, 32	1129.32	0.59	5	0.37	1.09	(205)	(154)	(402)
	34-2, 34	1129.34	0.71	6	0.85	0.67	60	94	411
N2	34-2, 36	1129.36	0.67	6	3.30	8.58	250	43	418
	34-2, 38	1129.38	0.55	5	4.44	14.47	311	49	416
	34-2, 40	1129.40	0.67	6	3.96	11.96	289	57	417
	34-2, 42	1129.42	0.86	7	5.00	17.60	336	39	415
	34-2, 44	1129.44	0.00	0	5.72	23.06	377	46	413
	34-2, 46	1129.46	0.54	4	5.98	25.33	398	58	415
	34-2, 48	1129.48	0.22	2	5.67	23.86	389	72	412
	34-2, 50	1129.50	0.54	4	5.52	23.44	394	65	410
	34-2, 52	1129.52	0.54	4	6.58	27.36	391	30	411
	34-2, 54	1129.54	0.31	3	4.13	14.52	332	73	412
	34-2, 56	1129.56	0.70	6	5.14	19.27	360	53	412
	34-2, 58	1129.58	0.67	6	3.94	16.56	395	43	413
	34-2, 60	1129.60	0.83	7	4.23	13.09	295	43	412
	34-2, 62	1129.62	0.23	2	1.19	0.68	49	159	412
	34-2, 64	1129.64	0.23	2	3.31	6.18	163	59	411
	34-2, 66	1129.66	0.94	8	6.28	29.98	453	20	416
	34-2, 68	1129.68	0.54	4	6.54	27.88	401	20	412
	34-2, 70	1129.70	0.54	4	5.98	23.86	379	21	411
	34-2, 72	1129.72	0.54	4	7.00	28.06	377	19	412
	34-2, 74	1129.74	0.30	2	7.59	31.92	394	18	411
	34-2, 76	1129.76	0.62	5	7.34	30.88	401	16	413
	34-2, 78	1129.78	0.54	4	5.63	22.62	374	20	412
	34-2, 80	1129.80	1.26	10	11.09	59.14	506	13	409
	34-2, 82	1129.82	1.02	8	8.71	39.04	424	15	410
	34-2, 84	1129.84	0.78	6	5.54	24.18	406	20	411
	34-2, 86	1129.86	1.02	8	8.66	38.96	422	14	410
	34-2, 88	1129.88	0.86	7	12.71	62.64	466	12	409
	34-2, 90	1129.90	0.86	7	6.87	28.30	387	17	412
	34-2, 92	1129.92	0.54	4	7.51	30.36	379	16	412
	34-2, 94	1129.94	0.62	5	7.90	33.90	399	15	411
	34-2, 96	1129.96	0.70	6	6.44	23.94	346	44	411
	34-2, 98	1129.98	0.78	6	6.00	22.70	363	46	415
	34-2, 100	1130.00	0.62	5	7.47	32.13	407	49	409
	34-2, 102	1130.02	0.38	3	1.47	1.79	99	105	418
N1	34-2, 104	1130.04	0.27	2	0.35	0.15	31	91	440
	34-2, 106	1130.06	0.35	3	0.58	0.47	64	59	410
M2	34-2, 108	1130.08	0.38	3	4.26	13.28	299	33	415
	34-2, 110	1130.10	0.79	7	4.35	14.84	325	37	415
	34-2, 112	1130.12	1.02	8	7.29	32.00	416	43	411
	34-2, 114	1130.14	1.02	8	7.35	36.28	470	49	413
	34-2, 116	1130.16	0.78	6	6.09	29.44	457	54	413
	34-2, 118	1130.18	0.62	5	5.80	24.10	387	64	410
	34-2, 120	1130.20	0.14	1	6.09	24.46	377	42	410
	34-2, 122	1130.22	0.86	7	7.04	29.92	398	53	412
	34-2, 124	1130.24	0.86	7	8.88	39.02	415	50	410
	34-2, 126	1130.26	1.26	10	9.76	45.74	438	50	410
	34-2, 128	1130.28	0.54	4	7.58	34.44	422	58	413
	34-2, 130	1130.30	1.10	9	14.58	68.39	437	45	410
	34-2, 132	1130.32	0.38	3	12.82	60.82	451	53	411
	34-2, 134	1130.34	0.46	4	11.29	52.72	441	56	409
	34-2, 136	1130.36	0.54	4	11.08	53.17	454	48	410
	34-2, 138	1130.38	0.70	6	8.22	37.99	435	56	413
	34-2, 140	1130.40	0.86	7	5.16	21.34	382	51	409
	34-2, 142	1130.42	0.55	5	4.39	17.20	354	65	410
	34-2, 144	1130.44	0.55	5	3.05	10.56	321	80	410
	34-2, 146	1130.46	0.43	4	3.38	5.88	163	80	411

Table 3 (continued).

Sedimentary Sequence	Core-Section (level in cm)	Sub-bottom depth (m)	Mineral carbon (%)	$CaCO_3$ (%)	TOC (%)	$S_1 + S_2$	HI	OI	T_{max}
	34-2, 148	1130.48	0.71	6	4.34	11.62	253	65	412
	34-3, 0	1130.50	0.39	3	4.00	10.10	238	42	413
	34-3, 2	1130.52	0.55	5	3.99	13.02	315	51	415
	34-3, 4	1130.54	0.47	4	1.49	1.16	74	94	419
M1	34-3, 6	1130.56	0.63	5	0.49	0.32	55	71	411
	34-3, 8	1130.58	0.07	1	0.50	0.28	48	96	410
	34-3, 10	1130.60	0.19	2	0.70	0.37	46	53	409
L2	34-3, 12	1130.62	0.94	8	7.15	30.54	404	41	414
	34-3, 14	1130.64	0.62	5	5.03	20.27	378	53	413
	34-3, 16	1130.66	0.38	3	7.15	29.79	394	48	414
	34-3, 18	1130.68	0.54	4	8.52	39.64	437	43	410
	34-3, 20	1130.70	1.02	8	7.49	30.85	390	33	413
	34-3, 22	1130.72	0.38	3	7.48	29.85	373	42	411
	34-3, 24	1130.74	0.38	3	5.27	22.86	407	59	411
	34-3, 26	1130.76	0.22	2	5.48	22.52	382	49	412
	34-3, 28	1130.78	0.30	2	5.27	21.34	376	39	414
	34-3, 30	1130.80	0.30	2	6.66	24.03	337	50	412
	34-3, 32	1130.82	0.30	2	8.98	39.32	415	63	414
	34-3, 34	1130.84	0.19	2	4.58	16.84	341	68	412
	34-3, 36	1130.86	0.23	2	5.18	14.59	263	31	408
	34-3, 38	1130.88	0.19	2	5.78	20.07	322	25	411
	34-3, 40	1130.90	0.23	2	5.86	21.47	338	24	409
	34-3, 42	1130.92	0.35	3	4.88	16.39	317	32	410
	34-3, 44	1130.94	0.35	3	3.46	9.82	272	20	414
	34-3, 46	1130.96	0.47	4	3.53	12.44	333	12	415
	34-3, 48	1130.98	0.43	4	4.10	16.27	371	32	412
	34-3, 50	1131.00	0.43	4	4.37	15.52	331	15	410
	34-3, 52	1131.02	0.43	4	3.45	10.79	288	19	410
	34-3, 54	1131.04	0.86	7	6.42	29.59	433	30	410
	34-3, 56	1131.06	0.46	4	7.16	25.30	335	39	409
	34-3, 58	1131.08	0.38	3	7.78	32.50	398	44	409
	34-3, 60	1131.10	0.62	5	11.58	55.20	453	41	410
	34-3, 62	1131.12	1.02	8	9.78	48.55	464	37	408
	34-3, 64	1131.14	0.46	4	14.40	67.00	440	44	406
	34-3, 66	1131.16	0.30	2	10.68	43.85	390	45	410
	34-3, 68	1131.18	0.62	5	10.50	47.15	429	41	410
	34-3, 70	1131.20	0.84	7	10.71	43.34	390	40	415
	34-3, 71	1131.21	0.62	5	10.26	42.80	396	47	411
	34-3, 72	1131.22	0.70	6	12.21	63.00	490	42	410
	34-3, 74	1131.24	0.38	3	9.50	42.90	429	47	411
	34-3, 76	1131.26	0.38	3	6.79	28.35	396	54	412
L1	34-3, 78	1131.28	0.07	1	0.29	0.57	(145)	(197)	(407)
	34-3, 80	1131.30	0.43	4	0.54	0.72	74	130	383
	34-3, 82	1131.32	0.43	4	1.00	0.82	67	65	414
	34-3, 84	1132.34	0.19	2	0.18	0.55	(139)	(444)	(348)
K2	34-3, 86	1131.36	0.23	2	2.21	4.35	183	48	414
	34-3, 88	1131.38	0.62	5	11.45	52.90	442	41	407
	34-3, 90	1131.40	0.19	2	0.70	2.12	181	421	339
	34-3, 92	1131.42	0.00	0	1.38	2.76	171	128	411
	34-3, 94	1131.44	0.07	1	1.52	3.96	204	175	411
	34-3, 96	1131.46	0.43	4	4.47	13.70	287	48	414
	34-3, 98	1131.48	0.11	1	1.45	3.04	153	191	410
	34-3, 100	1131.50	0.15	1	0.75	0.92	89	100	409
K1	34-3, 102	1131.52	0.23	2	0.21	0.21	52	167	367
	34-3, 104	1131.54	0.99	8	0.10	0.20	90	220	380
	34-3, 106	1131.56	0.43	4	0.26	0.17	27	162	367
	34-3, 108	1131.58	0.00	0	0.17	0.50	(176)	(659)	342
	34-3, 110	1131.60	0.00	0	0.18	0.12	44	128	375
J2	34-3, 112	1131.62	0.27	2	0.86	0.46	48	33	412
	34-3, 114	1131.64	0.27	2	0.76	0.32	34	34	415
	34-3, 116	1131.66	0.39	3	0.94	0.62	60	30	414
	34-3, 118	1131.68	2.58	21	1.19	1.07	86	31	415
	34-3, 120	1131.70	0.00	0	3.31	7.09	203	63	414
J1	34-3, 122	1131.72	0.15	1	0.32	0.74	(178)	(206)	(388)
I2	34-3, 124	1131.74	0.00	0	2.95	5.76	183	45	406
I1	34-3, 126	1131.76	0.27	2	0.27	0.22	44	81	405
	34-3, 128	1131.78	0.11	1	0.11	0.09	27	145	407
	34-3, 130	1131.80	0.15	1	0.13	0.07	8	46	0
	34-3, 132	1131.82	0.47	4	0.08	0.06	38	0	0
	34-3, 134	1131.84	0.31	3	0.05	0.09	(120)	(60)	(348)
	34-3, 136	1131.86	0.27	2	0.06	0.05	33	100	440
	34-3, 138	1131.88	0.54	4	8.88	36.58	393	34	409
	34-3, 140	1131.90	0.30	2	7.82	29.06	355	50	409
	34-3, 142	1131.92	0.30	2	6.93	20.56	280	56	409

Table 3 (continued).

Sedimentary Sequence	Core-Section (level in cm)	Sub-bottom depth (m)	Mineral carbon (%)	$CaCO_3$ (%)	TOC (%)	$S_1 + S_2$	HI	OI	T_{max}
	34-3, 144	1131.94	0.70	6	7.06	28.86	388	47	412
	34-3, 146	1131.96	0.30	2	8.35	31.73	360	47	412
	34-3, 148	1131.98	0.38	3	9.12	39.13	404	40	409
H2	34-4, 0	1132.00	0.46	4	6.67	23.83	336	49	411
	34-4, 2	1132.02	0.39	3	4.15	12.86	292	66	414
	34-4, 4	1132.04	0.31	3	2.68	6.43	224	91	415
	34-4, 6	1132.06	0.47	4	2.98	7.99	258	50	414
	34-4, 8	1132.08	0.47	4	2.80	8.71	294	43	411
	34-4, 10	1132.10	0.51	4	1.67	1.96	107	57	416
	34-4, 12	1132.12	0.31	3	1.43	1.57	101	67	413
	34-4, 14	1132.14	0.51	4	0.14	0.13	71	193	459
H1	34-4, 16	1132.16	0.79	7	0.27	0.09	22	107	375
	34-4, 18	1132.18	0.00	0	0.10	0.29	(210)	(270)	(393)
	34-4, 20	1132.20	0.59	5	0.28	0.17	50	64	410
	34-4, 22	1132.22	0.63	5	0.53	0.47	74	40	412
	34-4, 24	1132.24	0.63	5	0.93	0.46	40	44	409
	34-4, 26	1132.26	0.63	5	1.99	5.39	260	36	415
	34-4, 28	1132.28	0.67	6	0.37	0.24	59	57	412
G5	34-4, 30	1132.30	0.59	5	0.84	0.51	49	30	409
	34-4, 32	1132.32	0.71	6	0.91	0.46	43	38	412
	34-4, 34	1132.34	0.75	6	0.94	0.52	46	45	410
	34-4, 36	1132.36	0.63	5	0.42	0.19	33	62	410
	34-4, 38	1132.38	0.67	6	0.70	0.49	47	59	405
	34-4, 40	1132.40	0.75	6	0.96	0.53	45	54	408
	34-4, 42	1132.42	0.63	5	4.04	9.80	232	41	417
	34-4, 44	1132.44	0.67	6	3.47	7.16	196	47	418
	34-4, 46	1132.46	0.55	5	3.68	11.66	301	48	416
	34-4, 48	1132.48	0.47	4	3.44	9.36	257	49	413
	34-4, 50	1132.50	0.59	5	2.80	5.16	175	56	418
	34-4, 52	1132.52	0.63	5	2.53	4.60	171	58	416
	34-4, 54	1132.54	0.35	3	4.41	10.99	234	51	409
	34-4, 56	1132.56	0.78	6	6.50	26.54	390	43	413
	34-4, 58	1132.58	0.70	6	4.49	11.82	247	50	409
	34-4, 60	1132.60	0.70	6	5.01	15.78	296	50	411
G4	34-4, 62	1132.62	0.38	3	6.05	21.90	344	42	412
	34-4, 64	1132.64	0.70	6	5.83	22.16	366	50	411
	34-4, 66	1132.66	0.78	6	4.91	15.70	306	52	411
	34-4, 68	1132.68	0.78	6	5.26	17.94	323	49	409
	34-4, 70	1132.70	0.62	5	4.15	12.00	276	58	409
	34-4, 72	1132.72	0.54	4	4.29	12.06	269	57	410
	34-4, 74	1132.74	0.43	4	1.21	1.02	78	79	419
	34-4, 76	1132.76	0.47	4	1.22	1.18	90	67	421
	34-4, 78	1132.78	0.47	4	1.30	1.16	83	63	420
	34-4, 80	1132.80	0.55	5	1.30	1.08	78	65	421
	34-4, 82	1132.82	0.71	6	1.48	1.05	64	27	420
	34-4, 84	1132.84	0.71	6	0.51	0.14	14	35	402
	34-4, 86	1132.86	0.67	6	0.93	0.43	35	26	413
	34-4, 88	1132.88	0.59	5	0.84	0.45	36	33	411
	34-4, 90	1132.90	0.75	6	0.33	0.12	18	24	401
	34-4, 92	1132.92	0.63	5	0.40	0.14	20	38	404
G3	34-4, 94	1132.94	0.51	4	0.27	0.09	11	48	322
	34-4, 96	1132.96	0.59	5	0.53	1.00	19	28	398
	34-4, 98	1132.98	0.55	5	0.33	0.14	18	33	340
	34-4, 100	1133.00	0.71	6	0.27	0.17	37	15	408
	34-4, 102	1133.02	0.55	5	0.09	0.09	44	111	328
	34-4, 104	1133.04	0.47	4	0.07	0.13	(114)	(171)	(349)
G2	34-4, 106	1133.06	0.43	4	0.82	0.60	59	17	14
	34-4, 108	1133.08	0.43	4	0.86	0.60	58	33	412
G1	34-4, 110	1133.10	0.35	3	0.24	0.23	71	63	417
	34-4, 112	1133.12	0.39	3	0.28	0.20	57	4	416
	34-4, 114	1133.14	0.62	5	7.15	26.54	353	29	406
	34-4, 116	1133.16	0.30	2	4.78	16.84	334	34	410
	34-4, 118	1133.18	0.35	3	2.68	6.40	226	33	414
	34-4, 120	1133.20	0.38	3	7.70	31.52	388	31	410
	34-4, 122	1133.22	0.38	3	5.76	11.89	195	65	413
	34-4, 124	1133.24	0.30	2	6.80	20.96	291	46	412
	34-4, 126	1133.26	0.54	4	6.79	23.29	322	54	414
	34-4, 128	1133.28	0.62	5	6.84	28.26	387	47	410
	34-4, 130	1133.30	0.22	2	5.21	17.14	307	71	411
	34-4, 132	1133.32	0.06	0	5.60	19.18	321	48	414
F2	34-4, 134	1133.34	0.38	3	5.81	17.80	287	56	411
	34-4, 136	1133.36	0.19	2	4.45	14.02	295	92	412
	34-4, 138	1133.38	0.70	6	6.05	21.44	332	66	412
	34-5, 0	1133.50	0.63	5	2.83	6.26	207	108	416
	34-5, 2	1133.52	0.11	1	2.08	2.60	114	87	411
	34-5, 4	1133.54	0.51	4	2.78	6.02	203	81	414

Table 3 (continued).

Sedimentary Sequence	Core-Section (level in cm)	Sub-bottom depth (m)	Mineral carbon (%)	$CaCO_3$ (%)	TOC (%)	$S_1 + S_2$	HI	OI	T_{max}
	34-5, 6	1133.56	0.51	4	3.37	8.78	241	69	412
	34-5, 8	1133.58	0.39	3	4.73	14.44	285	71	410
	34-5, 10	1133.60	0.47	4	3.68	10.94	279	98	410
	34-5, 12	1133.62	0.19	2	1.27	1.56	110	90	418
	34-5, 14	1133.64	0.23	2	1.34	1.50	101	57	420
	34-5, 16	1133.66	0.31	3	1.23	1.48	107	46	417
F1	34-5, 18	1133.68	0.19	2	0.93	1.38	71	159	359
	34-5, 20	1133.70	0.94	8	5.25	18.09	324	39	415
	34-5, 22	1133.72	0.94	8	4.90	17.26	330	37	414
	34-5, 23	1133.73	0.90	7	7.79	28.86	355	30	416
	34-5, 24	1133.74	1.02	8	5.83	21.94	353	47	414
	34-5, 26	1133.76	0.78	6	5.68	20.13	337	70	415
	34-5, 28	1133.78	0.78	6	4.78	15.13	299	74	416
	34-5, 30	1133.80	1.10	9	3.51	13.69	374	49	419
	34-5, 32	1133.82	0.94	8	4.84	17.72	348	36	419
	34-5, 34	1133.84	0.78	6	4.73	16.86	341	32	419
E2	34-5, 36	1133.86	0.31	3	2.56	5.26	193	57	418
	34-5, 38	1133.88	0.51	4	1.97	3.24	152	46	417
	34-5, 40	1133.90	0.55	5	1.46	2.30	147	35	413
	34-5, 42	1133.92	0.55	5	1.52	2.23	136	39	415
	34-5, 44	1133.94	0.94	8	4.26	13.90	312	34	414
	34-5, 46	1133.96	1.02	8	4.91	17.88	351	34	418
	34-5, 48	1133.98	0.59	5	2.74	7.42	258	39	415
	34-5, 50	1134.00	0.94	8	3.91	13.33	327	38	413
	34-5, 52	1134.02	0.86	7	4.87	16.16	317	40	415
	34-5, 54	1134.04	0.31	3	1.30	1.27	85	82	412
	34-5, 56	1134.06	0.23	2	0.22	0.26	91	218	423
	34-5, 58	1134.08	0.39	3	0.37	0.28	68	138	450
E1	34-5, 60	1134.10	0.59	5	0.23	0.21	78	139	476
	34-5, 62	1134.12	0.43	4	0.18	0.31	(133)	(100)	(441)
	34-5, 64	1134.14	0.07	1	0.34	0.42	65	100	382
	34-5, 66	1134.16	0.39	3	2.06	3.64	169	52	418
D2	34-5, 68	1134.18	0.46	4	4.60	15.13	314	46	410
	34-5, 70	1134.20	0.70	6	5.29	18.19	328	48	410
	34-5, 72	1134.22	0.51	4	2.53	4.99	189	56	417
	34-5, 74	1134.24	0.43	4	0.35	0.19	43	177	424
D1	34-5, 76	1134.26	0.31	3	0.26	0.26	77	258	401
	34-5, 78	1134.28	0.15	1	0.41	0.24	46	168	410
C2	34-5, 80	1134.30	0.30	2	4.01	12.46	300	51	411
	34-5, 82	1134.32	0.46	4	4.63	17.00	354	47	411
C1	34-5, 84	1134.34	0.31	3	0.72	0.58	69	140	415
	34-5, 86	1134.36	0.23	2	0.50	0.40	58	108	405
B2	34-5, 88	1134.38	1.10	9	4.88	17.13	339	46	412
	34-5, 90	1134.40	0.43	4	0.42	0.23	36	176	407
	34-5, 92	1134.42	0.43	4	0.15	0.19	(107)	(173)	(453)
	34-5, 94	1134.44	0.51	4	0.23	0.24	83	148	468
	34-5, 96	1134.46	0.67	6	0.13	0.17	62	277	382
	34-5, 98	1134.48	0.63	5	0.16	0.22	69	238	393
	34-5, 100	1134.50	0.59	5	0.10	0.12	60	320	357
	34-5, 102	1134.52	0.59	5	0.21	0.19	38	148	321
	34-5, 104	1134.54	0.67	6	0.22	0.24	36	168	321
B1	34-5, 106	1134.56	0.59	5	0.12	0.11	67	283	383
	34-5, 108	1134.58	0.71	6	0.13	0.13	62	262	359
	34-5, 110	1134.60	0.59	5	0.16	0.19	75	238	469
	34-5, 112	1134.62	0.67	6	0.16	0.20	(106)	(250)	(475)
	34-5, 114	1134.64	0.95	8	0.18	0.17	56	100	431
	34-5, 116	1134.66	0.63	5	0.22	0.19	50	105	405
	34-5, 118	1134.68	0.71	6	0.11	0.06	36	118	362
	34-5, 120	1134.70	0.79	7	0.09	0.07	33	78	0
	34-5, 122	1134.72	0.83	7	0.12	0.08	17	117	318
	34-5, 124	1134.74	0.59	5	0.11	0.13	64	182	455
	34-5, 126	1134.76	0.71	6	1.29	0.80	54	45	422
	34-5, 128	1134.78	0.67	6	1.70	1.52	82	44	424
	34-5, 130	1134.80	0.39	3	1.04	0.64	50	50	419
	34-5, 132	1134.82	0.43	4	1.27	0.84	54	38	416
A4	34-5, 134	1134.84	0.35	3	1.21	0.72	51	51	418
	34-5, 136	1134.86	0.39	3	1.19	0.88	64	42	421
	34-5, 138	1134.88	0.39	3	1.36	1.02	57	38	418
	34-5, 140	1134.90	0.59	5	1.79	1.48	77	42	426
	34-5, 142	1134.92	0.67	6	1.13	0.52	41	44	420
	34-5, 144	1134.94	0.55	5	0.82	0.54	51	59	408
	34-5, 146	1134.96	0.59	5	0.51	0.30	47	51	418
	34-5, 148	1134.98	0.67	6	0.45	0.30	31	53	399
	34-6, 0	1135.00	0.67	6	0.31	0.35	52	77	379

Table 3 (continued).

Sedimentary Sequence	Core-Section (level in cm)	Sub-bottom depth (m)	Mineral carbon (%)	$CaCO_3$ (%)	TOC (%)	$S_1 + S_2$	HI	OI	T_{max}
	34-6, 2	1135.02	0.55	5	0.24	0.21	42	83	333
A3	34-6, 4	1135.04	0.59	5	0.44	0.33	55	55	411
	34-6, 6	1135.06	0.47	4	0.34	0.33	76	100	407
	34-6, 8	1135.08	0.51	4	0.46	0.36	52	67	405
	34-6, 10	1135.10	0.47	4	0.36	0.16	36	67	425
	34-6, 12	1135.12	0.47	4	0.26	0.19	58	81	413
A2	34-6, 14	1135.14	1.11	9	0.73	0.37	40	70	406
	34-6, 16	1135.16	0.31	3	0.74	0.39	42	53	404
	34-6, 18	1135.18	0.63	5	0.19	0.17	68	116	402
	34-6, 20	1135.20	0.51	4	0.30	0.59	(147)	(203)	(361)
	34-6, 24	1135.24	0.47	4	0.14	0.20	86	93	378
	34-6, 26	1135.26	0.67	6	0.13	0.17	85	115	385
	34-6, 28	1135.28	0.75	6	0.10	0.13	(110)	(170)	(411)
	34-6, 30	1135.30	0.59	5	0.17	0.29	65	118	324
	34-6, 32	1135.32	0.59	5	0.13	0.09	54	77	393
	34-6, 34	1135.34	0.51	4	0.15	0.17	73	93	370
	34-6, 36	1135.36	0.43	4	0.16	0.15	56	100	337
	34-6, 38	1135.38	0.63	5	0.12	0.18	75	75	361
	34-6, 40	1135.40	0.63	5	0.11	0.13	73	64	356
	34-6, 42	1135.42	0.55	5	0.11	0.11	55	100	334
	34-6, 44	1135.44	0.55	5	0.10	0.17	(120)	(210)	(387)
	34-6, 46	1135.46	0.39	3	0.08	0.13	(100)	(150)	(401)
	34-6, 48	1135.48	0.59	5	0.38	0.35	58	61	397
	35-1, 17	1136.67	0.39	3	0.59	0.43	47	51	392
	35-1, 26	1136.76	0.31	3	1.01	0.59	50	52	416
	35-1, 50	1137.00	0.35	3	1.65	0.98	53	41	422
A1	35-1, 70	1137.20	0.23	2	3.70	8.36	217	42	422
	35-1, 78	1137.28	0.31	3	1.86	2.15	105	49	420
	35-1, 113	1137.65	0.55	5	1.27	0.68	46	48	414
	35-2, 11	1138.11	0.43	4	1.20	0.60	45	40	423
	35-2, 24	1138.24	0.15	1	1.10	0.92	73	47	423
	35-2, 98	1138.98	0.31	3	0.96	0.68	65	54	424
	35-3, 3	1139.53	0.83	7	0.49	0.10	16	314	407
	35-3, 14	1139.64	0.19	2	0.96	0.80	71	33	420
	35-3, 44	1139.94	0.11	1	0.84	0.74	62	29	408
	35-3, 74	1140.24	0.69	6	2.74	5.01	177	91	430
	35-3, 75	1140.25	0.47	4	2.43	3.30	126	30	428
	35-3, 129	1140.79	0.43	4	1.17	0.48	32	22	416
	35-3, 149	1140.99	0.39	3	0.71	0.38	45	31	415
	35-4, 9	1141.09	0.79	7	0.40	0.20	30	85	359
	35-4, 38	1141.38	0.79	7	0.65	0.21	22	60	403
	35-4, 53	1141.53	0.63	5	0.97	0.36	28	42	411
	35-4, 86	1141.86	0.83	7	0.76	0.28	22	46	402
	35-4, 118	1142.18	0.51	4	0.95	0.75	63	47	416
	35-0, 16	1142.66	0.75	6	0.88	0.32	22	53	391

Note: Parentheses indicate doubtful data.

noflagellate cysts in the kerogen fraction. In Hole 603B the CTBE is composed of 19 sequences. At the bottom of the core (sequence A), the origin of the organic matter is identical to that of the underlying Hatteras Formation (terrestrial organic matter). However, the maximum TOC content reached in the sequences gradually increases with the petroleum potential and the hydrogen index. Each new sequence reaches higher values than the underlying one, up to sequence Q (Section 1, between 62 and 94 cm).

In Site 105, only 68 n. mi. farther southeast, the CTBE is thinner (only 1.5 m) but the maximum TOC content is the same (up to 25 wt.%).

The CTBE is not a single, homogeneous, black shale layer, but appears to be a condensation of several thin levels, richer and richer in organic matter of type II origin, interbedded with thinner levels of green claystones. The alternation is identical to that of the Hatteras Formation, but in the CTBE preservation of organic matter of marine origin is better, indicating the presence of an anoxic environment just before the multicolored claystones in the Plantagenet Formation were deposited.

The spreading of the CTBE off the American continental margin (Sites 105 and 603) shows that the phenomenon previously recognized off the African and European continental margins (Sites 135, 137, 138, 367, 398, and 551) is not restricted to the eastern North Atlantic. In addition, this type of sediment has even been observed on the continental margin of Venezuela in the La Luna and Querecual formations (Hedberg, 1937, 1950), where it is an effective source rock. The CTBE seems to be a general feature, not a local one, of the North and South Atlantic oceans and the Tethys (Thurow and Kuhnt, in press; Herbin, Montadert, et al., in press; Herbin, Müller, et al., in press).

No simple explanation can be given for the phenomenon. The initial factor could be the acceleration of seafloor spreading, with an increase in tectono-magmatic processes on the ridge and consequently a rise of the sea level according to Boer's model (1983). However, it has

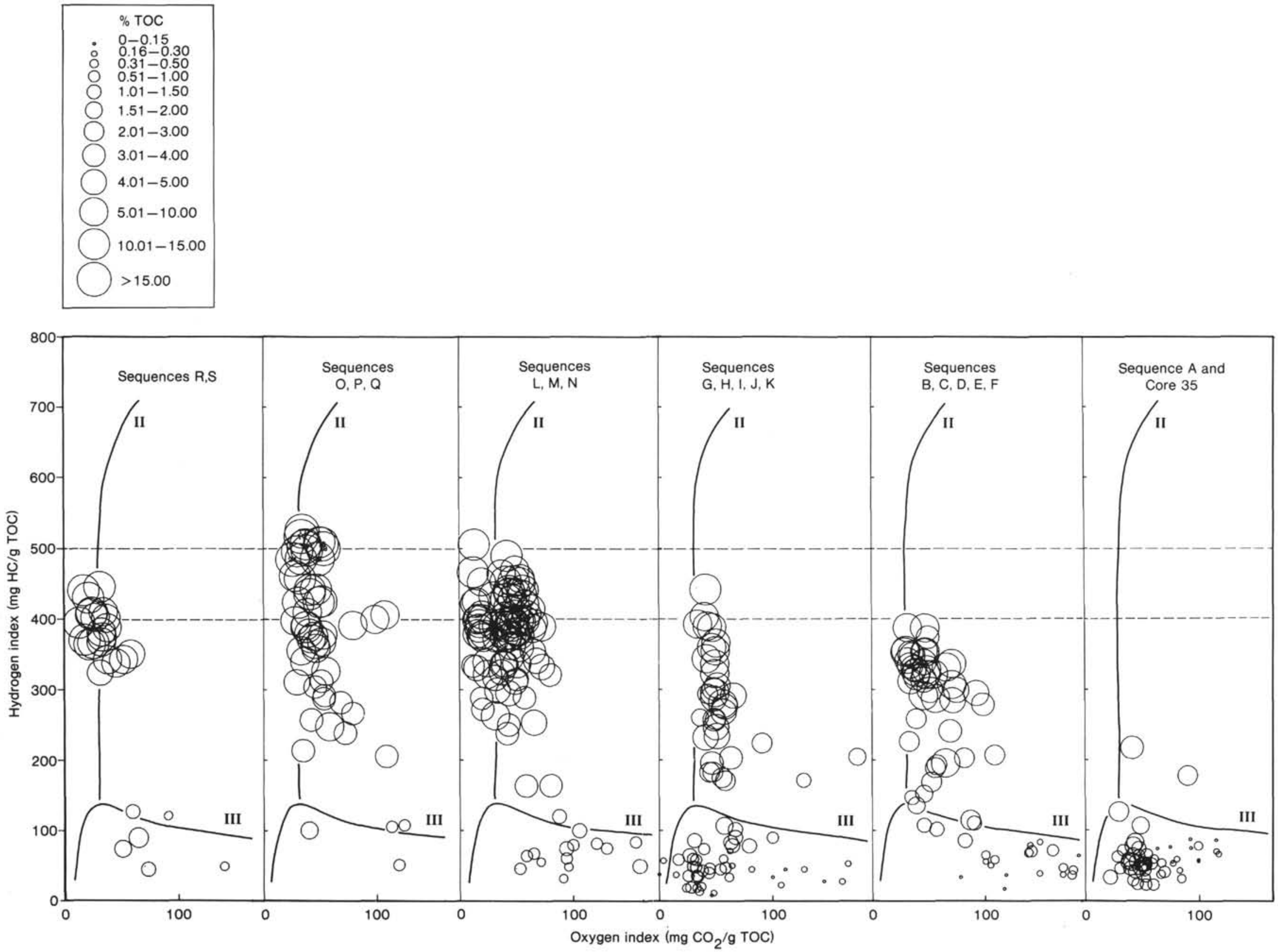

Figure 10. Characterization of the type of organic matter by pyrolysis method in the Cenomanian/Turonian Boundary Event at Site 603 (Sequences A to S, Sections 603B-34-1 to 603B-34-6 and 603B-35-1 to 603B-35-6). Size of the circles is proportional to total organic carbon.

not been truly settled whether the anoxic, deep ocean waters acted as an active trap or whether a relative increase in organic productivity in the ocean, too high for slow ocean water circulation, induced anoxia in deep water. But the hypothesis of high productivity is not truly in accordance with the low rate of sedimentation, and the reason that the ocean became more or less globally anoxic before the Plantagenet Formation was deposited still remains to be determined.

ACKNOWLEDGMENTS

The authors are indebted to Dr. George Claypool of the U.S. Geological Survey, Dr. Dean A. Dunn of the University of Southern Mississippi, and Drs. Warren S. Drugg and Robert W. Jones of the Chevron Oil Field Research Laboratory for comments upon and review of the present paper.

REFERENCES

Azéma, C., Fauconnier, D., and Viaud, M. J., 1981. Microfossils from the Upper Cretaceous of Vendée (France). *Rev. Palaeobot. Palynol.*, 35:237–281.

Below, R., 1981. Dinoflagellaten-Zysten aus dem oberen Hauterive bis unteren Cenoman Süd-West-Marokkos. *Palaeontographica, Abt. B*, 176:1–145.

———, 1982. Scolochorate Zysten der Gonyaulacaceae (Dinophyceae), aus der Unterkreide Marokkos. *Palaeontographica, Abt. B*, 182:1–51.

Boer, P. L. de, 1983. Aspects of middle Cretaceous pelagic sedimentation in Southern Europe; production and storage of organic matter, stable isotopes, and astronomical influences [Thesis]. Utrecht, Instituut voor Aardwetenschappen der Rijksuniversiteit.

Boltenhagen, E., 1977. Microplancton du Crétacé supérieur du Gabon. *Cah. Paléontol.*, pp. 1–150.

Bujak, J. P., and Davies, E. H., 1983. Modern and fossil Peridiniineae. *Am. Assoc. Stratigraphic Palynologists Contrib. Ser.*, 13:1–203.

Bujak, J. P., and Williams, G. L., 1978. *Cretaceous Palynostratigraphy of Offshore Southeastern Canada.* Geol. Surv. Canada, 297.

Chénet, P. Y., and Francheteau, J., 1979. Bathymetric reconstruction method: application to the Central Atlantic Basin between 10°N and 40°N. *In* Donnelly, T., Francheteau, J., Bryan, W., Robinson, P., Flower, M., Salisbury, M., et al., *Init. Repts. DSDP*, 51, 52, 53, Pt. 2: Washington (U.S. Govt. Printing Office), 1501–1514.

Cookson, I. C., and Hughes, N. F., 1964. Microplankton from the Cambridge Greensand (mid-Cretaceous). *Palaeontology*, 7:37–59.

Davey, R. J., 1969. Non-calcareous microplankton from the Cenomanian of England, northern France and North America; Part 1. *Bull. Brit. Mus. (Nat. Hist.), Geol.*, 7:103–180.

Davey, R. J., and Verdier, J. P., 1973. An investigation of microplankton assemblages from latest (Vraconian) sediments. *Rev. Espan. Micropaleontol.*, 5:173–212.

———, 1976. A review of certain non-tabulate Cretaceous hystrichospherid dinocysts. *Rev. Palaeobot. Palynol.*, 22:307–335.

Espitalié, J., Deroo, G., and Marquis, F. 1985. La pyrolyse Rock-Eval et ses applications. *Rev. Inst. Franç. du Petrol.*, 40(5):563–579 (Pt. 1), 40(6):755–784 (Pt. 2), 41(1):73–89 (Pt. 3).

Espitalié, J., Laporte, J. L., Madec, M., Marquis, F., Leplat, P., and Paulet, J., 1977. Méthode rapide de caractérisation des roches mères, de leur potentiel pétrolier et de leur degré d'évolution. *Rev. Inst. Franç. du Petrol.*, 32(1):23–43.

Espitalié, J., Marquis, F., and Barsony, I., 1984. Geochemical logging. *In* Voorhees, K. J. (Ed.), *Analytical Pyrolysis Techniques and Applications:* London (Butterworth), pp. 276–304.

Ewing, J. I., and Hollister, C. D., 1972. Regional aspects of Deep Sea Drilling in the Western North Atlantic. *In* Hollister, C. D., Ewing, J. I., et al., *Init. Repts., DSDP*, 11: Washington (U.S. Govt. Printing Office), 951–973.

Foucher, J. C., 1979. Distribution stratigraphique des kystes de Dinoflagellés et des Acritarches dans le Crétracé supérieur du Bassin de Paris et de l'Europe septentrionale. *Palaeontographica, Abt. B*, 169:78–105.

———, 1982. Dinoflagellés et Acritarches de Civray. *Bull. Cent. Rech. Explor.-Product. Elf Aquitaine*, 6(1):171–173.

Graciansky, P. C. de, Brosse, E., Deroo, G., Herbin, J. P., Montadert, L., Müller, C., Schaaf, A., and Sigal, J., 1982. Les formations d'âge Crétacé de l'Atlantique Nord et leur matiére organique, paléogéographie et milieux de dépôt. *Rev. Inst. Franç. Pet.*, 37:(3): 275–337.

Habib, D., 1972. Dinoflagellate stratigraphy, Leg XI, Deep Sea Drilling Project. *In* Hollister, C. D., Ewing, J. I., et al., *Init. Repts. DSDP*, 11: Washington (U.S. Govt. Printing Office), 367–426.

———, 1977. Comparison of Lower and middle Cretaceous palynostratigraphic zonations in the western North Atlantic. *In* Swain, F. M. (Ed.), *Stratigraphic Micropaleontology of Atlantic Basin and Borderlands*: New York (Elsevier), pp. 341–367.

Habib, D., and Drugg, W. S., 1983. Dinoflagellate age of Middle Jurassic–Early Cretaceous sediments in the Blake-Bahama Basin. *In* Sheridan, R. E., Gradstein, F. M., et al., *Init. Repts. DSDP*, 76: Washington (U.S. Govt. Printing Office), 623–638.

Habib, D., and Knapp, S., 1982. Stratigraphic utility of Cretaceous small acritarchs. *Micropaleontology*, 28(4):335–371.

Hedberg, H. D., 1937. Stratigraphy of the Rio Querecual section of northeastern Venezuela. *Geol. Soc. Am. Bull.*, 8:1971–2204.

———, 1950. Geology of eastern Venezuela. *Geol. Soc. Am. Bull.*, 61:1173–1215.

Herbin, J. P., and Deroo, G., 1982. Sédimentologie de la matiére organique dans les formations du Mésozoique de l'Atlantique Nord. *Bull Soc. Geol. France, 7éme série*, 24(3):497–510.

Herbin, J. P., Deroo, G., and Roucaché, J., 1983. Organic geochemistry in the Mesozoic and Cenozoic formations of Site 534, Leg 76, Blake-Bahama Basin, and comparison with Site 391, Leg 44. *In* Sheridan, R. E., Gradstein, F. M., et al., *Init. Repts. DSDP*, 76: Washington (U.S. Govt. Printing Office), 481–493.

Herbin, J. P., Montadert, L., Müller, C., Gomez, R., Thurow, J., and Wiedmann, J., in press. Organic-rich sedimentation at the Cenomanian/Turonian boundary in oceanic and coastal basins in the North Atlantic and Tethys. Summerhayes, C., and Shackleton, N. J. (Eds.), *North Atlantic Palaeoceanography*. Geol. Soc. London, Spec. Publ.

Herbin, J. P., Müller, C., Graciansky, P. C. de, Jacquin, T., Magniez, F., and Unternehr, P., in press. Cretaceous anoxic events in the South Atlantic. *Evoluçaâo do Atlântico Sul no Mesozoico*, IX Congresso Brasileiro de Paleontologia, Boletin Técnico da Petrobras.

Huc, A. Y., Durand, B., and Monin, J. C., 1978. Humic compounds and kerogens in cores from Black Sea sediments, Leg 42B, Holes 379A, B, and 380A. *In* Ross, D. A., Neprochnov, Y. P., et al., *Init. Repts. DSDP*, 42, Pt. 2: Washington (U.S. Govt. Printing Office), 737–748.

Ikan, R., Baedecker, M. J., and Kaplan, I. R., 1975a. Thermal alteration experiments on organic matter in recent marine sediment. II Isoprenoids. *Geochim Cosmochim. Acta.*, 39:187–194.

———, 1975b. Thermal alteration experiments on organic matter in recent marine sediment. III Aliphatic and steroidal alcohols. *Geochim. Cosmochim. Acta.*, 39:195–203.

Lancelot, Y., Hathaway, J. C., and Hollister, C. D., 1972. Lithology of sediments from the Western North Atlantic, Leg XI, Deep Sea Drilling Project. *In* Hollister, C. D., Ewing, J. I., et al., *Init. Repts. DSDP*, 11: Washington (U.S. Govt. Printing Office), 901–950.

Lentin, J. K., and Williams, G. L., 1981. *Fossil Dinoflagellates: Index to Genera and Species* (1981 Ed.). Bedford Inst. Oceangr. Rept., B1-R-81-12.

Manum, S., and Cookson, I. C., 1964. Cretaceous microplankton in a sample from Graham Island, Arctic Canada, collected during the second "Fram" Expedition (1898–1902). With notes on microplankton from the Hassel Formation, Ellef Ringnes Island. *Schrift. Norske Videnskaps-Akad. Oslo, I. Mat-Naturv. Klasse, Ny Ser.*, 17:1–35.

Masure, E., 1984. L'indice de diversité et les dominances des "communautés" de kystes de Dinoflagellés: marqueurs bathymétriques; forage 398D, croisiére 47B. *Bull. Soc. Géol. France, 7eme Ser.*, 26(1):93–111.

Morgan, R., 1978. Albian to Senonian palynology of Site 364, Angola Basin. *In* Bolli, H. M., Ryan, W. B. F., et al., *Init. Repts. DSDP*, 40: Washington (U.S. Govt. Printing Office), 915–951.

Müller, C., Schaff, A., and Sigal, J., 1983. Biochronostratigraphie des formations d'âge Crétacé dans les forages du DSDP dans l'Océan Atlantique Nord. *Rev. Inst. Franç. Pet.*, 38(6): 683–708, 39(1):3–23.

Roucaché, J., Deroo, G., and Boulet, R., 1979. Caractérisation par différentes méthodes physico-chimiques de types de matiére organique dans des sédiments du Crétacé d'Atlantique en mer profonde. *Rev. Inst. Franç. Pet.*, 34(2):191–220.

Sever, J., Parker, P. L., 1969. Fatty alcohols (normal and isoprenoid) in sediments. *Science*, 164:1052–1054.

Simoneit, B. R. T., 1973. Appendix I: The identification of isoprenoidal ketones in Deep Sea Drilling Project core samples and their geochemical significance. *In* Burns, R. E., Andrews, J. E., et al., *Init. Repts. DSDP*, 21: Washington (U.S. Govt. Printing Office), 909–931.

Thurow, J., and Kuhnt, W., in press. Mid-Cretaceous of the Gibraltar Arch Area—organic-carbon-rich sediments, faunal patterns, palaeoenvironment. An attempt to continue off-shore to on-shore outcrops. *In* Summerhayes, C., and Shackleton, N. J. (Eds.), *North Atlantic Palaeoceanography.* Geol. Soc. London, Spec. Publ.

Tissot, B., Deroo, G., and Herbin, J. P., 1979. Organic matter in Cretaceous sediments of the North Atlantic. Talwani, M., Hay, W., Ryan, W. B. F. (Eds.), *Deep Drilling Results in the Atlantic Ocean*. Am. Geophys. Un., Maurice Ewing Series, 3:362–374.

Tissot, B., Durand, B., Espitalié, J., and Combaz, A., 1974. Influence of the nature and diagenesis of organic matter in the formation of petroleum *Am. Assoc. Pet. Geol. Bull.*, 58:499–506.

Tissot, B., and Pelet, R., 1981. Source and fate of organic matter in ocean sediments. *Oceanol. Acta, Actes 26 Int. Congr. Geol., Paris*, pp. 97–103.

Date of Initial Receipt: 21 February 1985
Date of Acceptance: 7 November 1985

APPENDIX
Palynomorph Species

Achomosphaera triangulata (Gerlach, 1961) Davey and Williams, 1969
Adnatosphaeridium apenninicum Corradini, 1972 (Plate 2, Fig. 8)
Callaisosphaeridium asymmetricum (Deflandre and Courteville, 1939) Davey and Williams, 1966
Chatangiella manumii (Vozzhennikova, 1967) Lentin and Williams, 1976 (Plate 2, Fig. 3)
Chatangiella sp. (Plate 2, Fig. 7)
Chichaouadinium vestitum (Brideaux, 1971) Bujak and Davies, 1983 (Plate 1, Fig. 12)
Coronifera striolata (Deflandre, 1937) Stover and Evitt, 1978 (Plate 2, Fig. 5)
Coronifera oceanica Cookson and Eisenack, 1958
Cyclonephelium distinctum Deflandre and Cookson, 1955
Cyclonephelium hughesii Clarke and Verdier, 1967 (Plate 1, Fig. 8)
Cyclophelium membraniphorum Cookson and Eisenack, 1962 (Plate 1, Fig. 5)
Cyclonephelium vannophorum Davey, 1969
Dinogymnium acuminatum Evitt et al., 1967 (Plate 1, Fig. 7)
Dinogymnium euclaense Cookson and Eisenack, 1970
Dinopterygium cladoides Deflandre, 1935
Dissiliodinium globulum Drugg, 1978
Epelidosphaeridia spinosa (Cookson and Hughes, 1964) Davey, 1969 (Plate 1, Fig. 1)
Exochosphaeridium bifidum (Clarke and Verdier, 1967) Clarke et al., 1968
Exochosphaeridium phragmites Davies et al., 1966
Florentinia cooksoniae (Singh, 1971) Duxbury, 1980
Florentinia radiculata (Davey and Williams, 1966) Davey and Verdier, 1973
Florentinia resex Davey and Verdier, 1976 (Plate 1, Fig. 11)
Heterosphaeridium heteracanthum (Deflandre and Cookson, 1955) Eisenack and Kjellström, 1971
Hystrichodinium pulchrum Deflandre, 1935
Hystrichosphaeridium palmatum (White, 1842 ex Brown, 1848) Downie and Sarjeant, 1965
Isabelidinium sp.
Kiokansium polypes (Cookson and Eisenack, 1962) Below, 1982
Kleithriasphaeridium loffrense Davey and Verdier, 1976
Litosphaeridium siphonophorum (Cookson and Eisenack, 1958) Davey and Williams, 1966 (Plate 1, Fig. 2)
Odontochitina costata Alberti, 1961 (Plate 1, Fig. 3)
Odontochitina operculata (O. Wetzel, 1933) Deflandre and Cookson, 1955
Odontochitina porifera Cookson, 1956 (Plate 2, Fig. 4)
Oligosphaeridium complex (White, 1842) Davey and Williams, 1966
Oligosphaeridium dictyophorum (Cookson and Eisenack, 1958) Davey and Williams, 1969
Ovoidinium ovale (Cookson and Eisenack, 1970) Lentin and Williams, 1976 (Plate 1, Fig. 4)
Palaeohystrichophora infusorioides Deflandre, 1935 (Plate 1, Fig. 9)
Palaeoperidinium cretaceum Pocock, 1962
Polysphaeridium ambiguum (Deflandre, 1937) Yun, 1981
Pterospermella australiensis (Deflandre and Cookson, 1955) Eisenack, 1972
Psaligonyaulax deflandrei Sarjeant, 1966
Rottnestia borussica (Eisenack, 1954) Cookson and Eisenack, 1961 (Plate 2, Fig. 6)
Senoniasphaera protrusa Clarke and Verdier, 1967 (Plate 2, Fig. 2)
Senoniasphaera rotundata Clarke and Verdier, 1967 (Plate 2, Fig. 1)
Spinidinium lanternum Cookson and Eisenack, 1970 (Plate 2, Fig. 9)
Spiniferites ancoriferum Cookson and Eisenack, 1974
Spiniferites cingulatus ssp. *cingulatus* (O. Wetzel, 1933) Lentin and Williams, 1973
Spiniferites crassipellis (Deflandre and Cookson, 1955) Sarjeant, 1970
Spiniferites ramosus ssp. *multibrevis* (Davey and Williams, 1966) Lentin and Williams, 1972
Subtilisphaera cheit Below, 1981 (Plate 1, Fig. 6)
Surculosphaeridium? longifurcatum (Firtion, 1952) Davey et al., 1966
Tanyosphaeridium variecalamum Davey and Williams, 1966
Trichodinium castenea (Deflandre, 1935) Clarke and Verdier, 1967
Trithyrodinium suspectum (Manum and Cookson, 1964) Davey, 1969 (Plate 1, Fig. 13)
Tubulospinosa oblongata Davey, 1970
Wallodinium sp.
Xenascus ceratioides (Deflandre, 1937) Lentin and Williams, 1973
Xiphophoridium alatum (Cookson and Eisenack, 1962) Sarjeant, 1966
Cyst. A (Plate 1, Fig. 10)

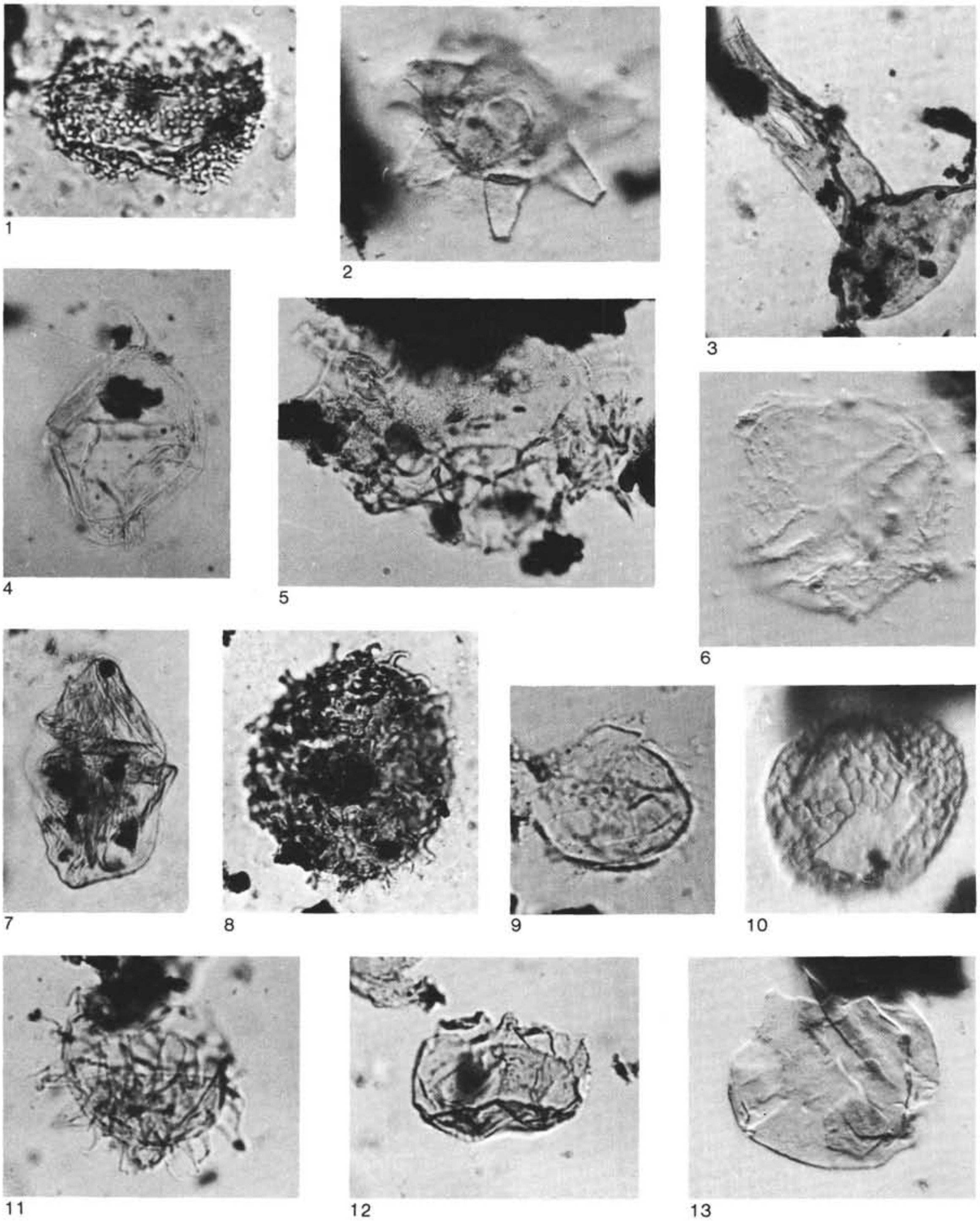

Plate 1. **1.** *Epelidosphaeridia spinosa* (Cookson and Hughes, 1964) Davey, 1969. Sample 603B-34-5, 23 cm. Slide no. 2, position England Finder Graticule (EFG): Q54, width 45 μm. **2.** *Litosphaeridium siphonophorum* (Cookson and Eisenack, 1958) Davey and Williams, 1966. Sample 603B-34-5, 23 cm. Slide no. 2, position EFG: Q33–34, width 52 μm. **3.** *Odontochitina costata* Alberti, 1961. Sample 603B-34-5, 23 cm. Slide no. 1, position EFG: K51, width 61 μm, height 100 μm. **4.** *Ovoidinium ovale* (Cookson and Eisenack, 1970) Lentin and Williams, 1976. Sample 603B-34-5, 23 cm. Slide no. 2, position EFG: E57, height 55 μm, width 36 μm. **5.** *Cyclonephelium membraniphorum* Cookson and Eisenack, 1962. Sample 603B-34-3, 70 cm. Slide no. 3, position EFG: Q33, width 77 μm. **6.** *Subtilisphaera cheit* Below, 1981. Sample 603B-34-3, 70 cm. Slide no. 4, position EFG: S36, height 56 μm, width 50 μm. **7.** *Dinogymnium acuminatum* Evitt et al., 1967. Sample 603B-34-3, 70 cm. Slide no. 5, position EFG: XY41, height 54 μm, width 30 μm. **8.** *Cyclonephelium hughesii* Clarke and Verdier, 1967. Sample 603B-34-5, 23 cm. Slide no. 3, position EFG: WX56–57, height 74 μm, width 68 μm. **9.** *Palaeohystrichophora infusorioides* Deflandre, 1935. Sample 603B-34-3, 70 cm. Slide no. 1, position EFG: N45-46, height 42 μm, width 35 μm. **10.** Cyst A. Sample 603B-34-3, 70 cm. Slide no. 1, position EFG: F50, width 43–40 μm. 3I archeopyle with quadra 2a. **11.** *Florentinia resex* Davey and Verdier, 1976. Sample 603B-33CC (1 cm). Slide no. 3, position EFG; S46, height 45 μm, width 50 μm. **12.** *Chichaouadinium vestitum* (Brideaux, 1971) Bujak and Davies, 1983. Sample 603B-33,CC, (1 cm). Slide no. 3, position EFG: V40, width 40 μm. I3Pa archeopyle. **13.** *Trithyrodinium suspectum* (Manum and Cookson, 1964) Davey, 1969. Sample 603B-33,CC (1 cm). Slide no. 2, position EFG: TU41–42, height 51 μm, width 45 μm.

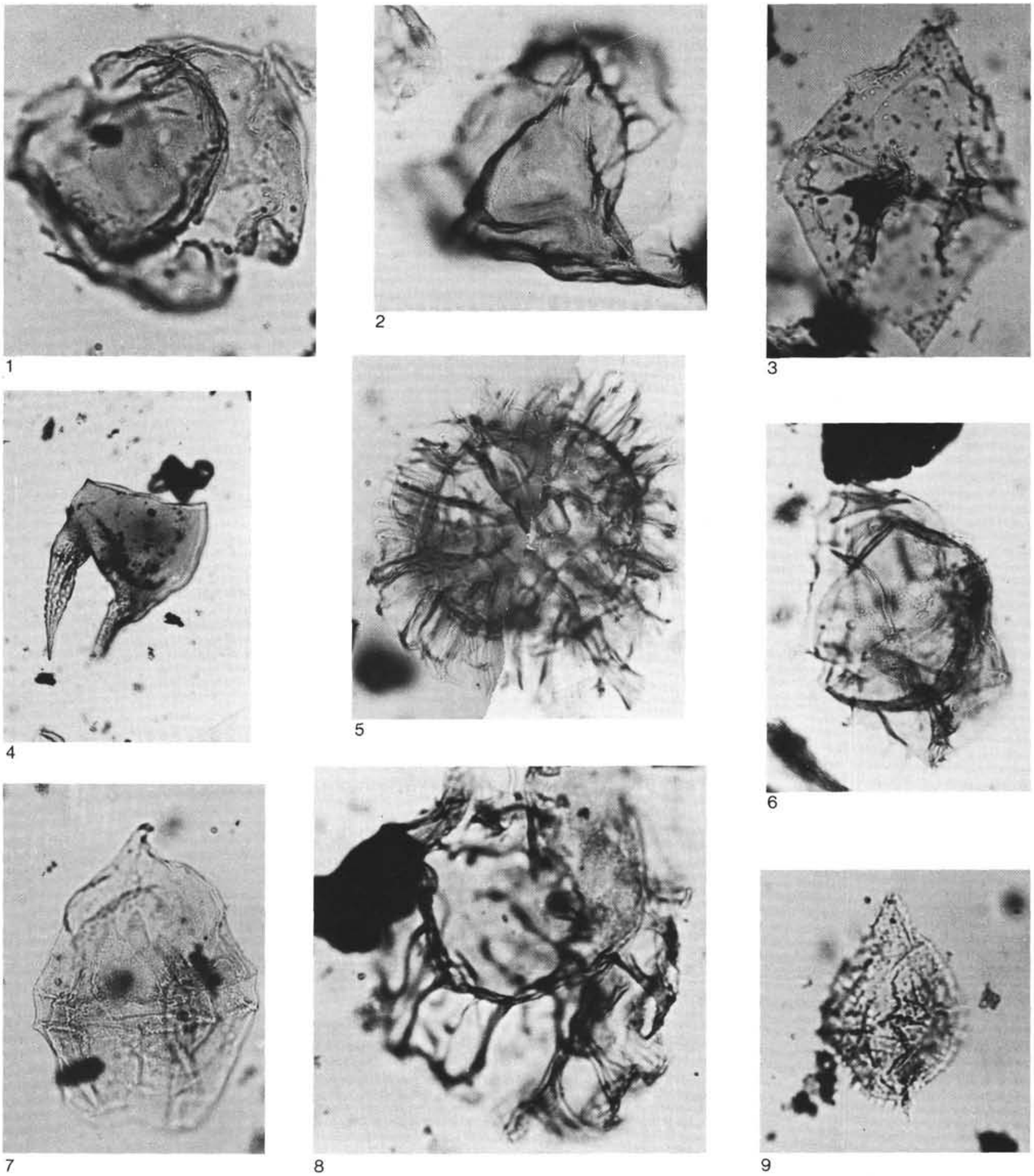

Plate 2. **1.** *Senoniasphaera rotundata* Clarke and Verdier, 1967. Sample 603B-29-1, 57 cm. Slide no. 1, position EFG: CD49, height 63 μm, endocyst diameter 45 μm. **2.** *Senoniasphaera protrusa* Clarke and Verdier, 1967. Sample 603B-29-1, 57 cm. Slide no. 2, position EFG: GH34, height 60 μm, endocyst height 45 μm, width 50 μm. **3.** *Chatangiella manumii* (Vozzhennikova, 1967) Lentin and Williams, 1976. Sample 603B-29-1, 57 cm. Slide no. 2, position EFG: B42, height 60 μm, width 45 μm, endocyst diameter 40 μm. **4.** *Odontochitina porifera* Cookson, 1956. Sample 603B-29-1, 57 cm. Slide no. 1, position EFG: L53–54, endocyst diameter 73 μm. **5.** *Coronifera striolata* (Deflandre, 1937) Stover and Evitt, 1978. Sample 603B-29-1, 57 cm. Slide no. 2, position EFG: NO40, height 75 μm, width 70 μm, endocyst diameter 46 μm. **6.** *Rottnestia borussica* (Eisenack, 1954) Cookson and Eisenack, 1961. Sample 603B-29-1, 57 cm. Slide no. 1, position EFG: X33, height 62 μm, width 45 μm. **7.** *Chatangiella* sp. Sample 603B-29-1, 57 cm. Slide no. 1, position EFG: UV38–39, height 64 μm, width 47 μm. **8.** *Adnatosphaeridium apenninicum* Corradini, 1972. Sample 603B-29-1, 57 cm. Slide no. 2, position EFG: M45-3, endocyst diameter 50 μm, processus height 23–25 μm, width 3–4 μm. **9.** *Spinidinium lanternum* Cookson and Eisenack, 1970. Sample 603B-29-1, 57 cm. Slide no. 1, position EFG: UV38–39, height 55 μm, width 30 μm.